IEEE Access
Multidisciplinary | Rapid Review | Open Access Journal

Received August 20, 2018, accepted November 12, 2018, date of publication November 20, 2018,
date of current version December 19, 2018.

Digital Object Identifier 10.1109/ACCESS.2018.2882491

Active Control of Chatter in Milling Process Using Intelligent PD/PID Control

SATYAM PAUL AND RUBEN MORALES-MENENDEZ
School of Engineering and Science, Tecnológico de Monterrey, Monterrey 64849, Mexico
Corresponding author: Satyam Paul (satyam.controlsystems@gmail.com)

This work was supported by the Tecnológico de Monterrey, Monterrey, Mexico.

ABSTRACT Chatter is an obstacle for achieving high-quality machining process and high production rate in industries. Chatter is an unstable self-exciting phenomenon that leads to tool wear, poor surface finish, and downgrade the milling operations. A novel active control strategy to attenuate the chatter vibration is proposed. *PD/PID* controllers in combination with Type-2 Fuzzy logic were utilized as a control strategy. The main control actions were generated by *PD/PID* controllers, whereas the Type-2 Fuzzy logic system was used to compensate the involved nonlinearities. The Lyapunov stability analysis was utilized to validate the stability of Fuzzy *PD/PID* controllers. The theoretical concepts and results are proved using numerical simulations. Although *PD/PID* controllers have been used for chatter control in machining process, the importance of stability along with the implementation of Type-2 Fuzzy logic system for nonlinearity compensation was the main contribution. In addition, active control using an *Active Vibration Damper* placed in an effective position is entirely a new approach with promising practical results.

INDEX TERMS Vibration control, manufacturing, fuzzy control, PD control, Lyapunov methods, stability analysis, control nonlinearities

I. INTRODUCTION

In all modern manufacturing industries, one of the most key feature is cutting process, although it results in self-excited vibrations having negative impacts [29]. Chatter is an important phenomena in machining process that affects the machining productivity by inducing low dimensional accuracy and reduction in the *Material Removal Rate* (*MRR*). It also results in below average surface finish as well as significant tool wear [26]. The consequences of milling chatter is that it generates large tool vibrations, minimizes tool life and hence reduces the quality and productivity of the process. Surface roughness is greatly affected by the large vibrations induced by the milling chatter thus resulting in improper finishing, less productivity and increased production time, [37]. Table 1 summarizes the acronym definitions.

The methodologies for chatter control can be categorized in three levels. The first methodology is to choose suitable machining parameters such as speed of the spindle and width of cut considering *Stability Lobe Diagram* (*SLD*). The main technique is to discard the chatter phenomena by selecting the machining parameters from outside the lobes [10]. There is a necessity of precise process parameters to calculate the lobe and hence the region of stabilized operation cannot be expanded via this technique, [41]. The second methodology is to disturb the effect of regeneration by changing the machining parameters continuously. *Spindle Speed Variation* (*SSV*) is a methodology related to this category that generates a time varying delay thus suppressing inconvenient phase lags between inner and outer chip modulation reducing chatter vibrations [38]. The third methodology is to alter the dynamics of machine tools by using additional passive or active devices to expand the chatter boundary.

The technique involving passive devices like *Dynamic Vibration Absorber* (*DVA*) and *Tuned Mass Damper* (*TMD*) have been exhaustively utilized for the minimization of chatter vibrations [33]. The design and implementation of a 2-*Degree of Freedom* (*DoF*). *TMD* for attenuation of milling chatter was investigated in [40]. The main advantages of passive devices are: the low cost and easy implementation. Also, it rules out the disadvantage of making the system destabilized. But, the main limitations are that the dampers require special methodologies for the validation of precise tuning of their natural frequencies for suitable performance. These passive devices are not adaptable to the varying machining conditions and they lack robustness.

The machine tool performance can be suitably improved by the technique of active control systems, which includes appropriate sensors and dampers installed on the spindle or tool holder [27]. An active damping controller with the technique of direct velocity feedback is proposed in [12].

TABLE 1. Acronym definitions.

Acronym	Definition
AVD	Active Vibration Damper
DoF	Degree of Freedom
DVA	Dynamic Vibration Absorber
FLS	Fuzzy Logic System
FoU	Footprint of Uncertainty
HSM	High Speed Machining
LCG	Linear Cuadratic Gaussian
MRR	Material Removal Rate
PD	Proportional Derivative
PID	Proportional Integral Derivative
SLD	Stability Lobe Diagram
SSV	Spindle Speed Variation
TMD	Tuned Mass Damper

A mechatronic simulator was used to validate the effectiveness of the controller. The technology of active damping of chatter with experimental validation has been researched in [13].

Reference [8] implemented an active damper system on a milling spindle associated with two orthogonal pairs of electrostrictive stack. A *Linear-Quadratic-Gaussian* (*LQG*) control law was developed to maintain a superior balance between performance and robustness. Reference [42] proposed an active model predictive control method to attenuate chatter with incorporated input constraints. Reference [6] proposed an adaptive active control approach to deal with the regenerative effect for *High Speed Machining* (*HSM*).

The main features for an effective controller are simple, robust, and fault tolerant. *Proportional* + *Derivative* (*PD*) and *Proportional* + *Integral* + *Derivative* (*PID*) controllers have been vastly utilized in industrial applications and processes. These controllers have superior effectiveness and robustness, when the knowledge of the model is missed, and also because of their simple nature with distinct physical meanings. The methodology of active elimination of chatter vibrations in milling via harmonic excitation of a workpiece was proposed in [39]. The system was developed on the basis of closed-loop control system, which is realized by a *PD* controller and is tested considering 2-*DoF* milling system. Also, a *PID* controller design was proposed in [1] for the mitigation of the chatter in milling process.

The phenomena of size effect leads to nonlinearity in the cutting force model [21]. Therefore, the consideration of nonlinearity in a cutting force model is crucial and must not be avoided for the precise prediction of the dynamic behavior of a milling system [9], [14], [34]. Recent research reveals that nonlinear modeling of the chatter phenomenon has widely been investigated as well as delayed nonlinear models having square and cubic polynomial terms associated to cutting force are taken into consideration, [23].

A Type-1 Fuzzy logic approach for chatter suppression in end milling processes was investigated in [17]. Reference [31] have investigated the chatter stability associated with milling processes using a Type-1 Fuzzy logic algorithm for compensation of uncertainty in this manufacturing process. Exhaustive investigation reveals that in comparison with the conventional Type-1 Fuzzy logic, Type-2 Fuzzy set demonstrates superior performance because of its integrated additional *DoF* termed to be as *Footprint of Uncertainty* (*FoU*), [4], [22]. The detailed concept and approach of Type-2 Fuzzy sets has been proposed in [16]. The Type-2 Fuzzy system is an efficient way to handle knowledge uncertainty in comparison to classical Type-1 Fuzzy logic as the Type-2 Fuzzy sets can handle uncertainties with more parameters as well as more design *DoF* [30]. This is one of the main contribution of this research.

The third method involving active control of chatter is carried out. First, the mathematical modeling of milling process along x and y component is accomplished. The nonlinearities incorporated in the process are identified and compensated through the Type-2 Fuzzy logic approach. The suppression of chatter is done by simulating the real effect of *Active Vibration Damper* (*AVD*). In the modeling equation, the dynamics of *AVD* is considered. The control action is carried out using the Proportional Derivative/Proportional Integral Derivative (*PD*/*PID*) strategy, which is utilized for chatter suppression. Second, the validation of stability criteria of the controllers is considered. Theorems are laid down thus validating various parameters condition and boundedness of the system states of the closed-loop system. Lyapunov stability candidate is exploited for the procedure. Third, using the designed *PD*/*PID* strategy with Type-2 Fuzzy in combination with *AVD*, the chatter suppression is achieved. An intensive numerical simulation analysis is carried out for the validation of theoretical concept and stability criteria. The entire control scheme implemented in this work have been illustrated by Fig. 1.

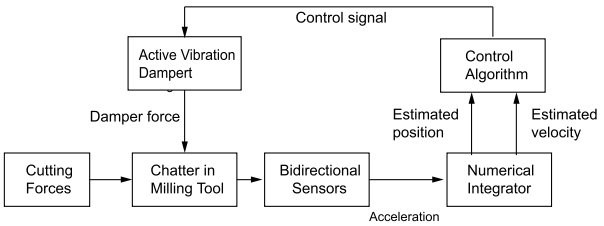

FIGURE 1. Control scheme for chatter control.

II. MODELING OF MILLING PROCESS WITH ACTIVE CONTROL

A general 2-*DoF* model of a milling process considering that the tool having n evenly spaced teeth and relatively flexible to the rigid workpiece is [19], [43]:

$$M\ddot{\mathbf{x}}(t) + C\dot{\mathbf{x}}(t) + K\mathbf{x}(t) = \mathbf{F}(\mathbf{t}) \quad (1)$$

where $M \in \Re^{2\times2}$, $C \in \Re^{2\times2}$ and $K \in \Re^{2\times2}$ are the mass, damping and stiffness matrices which are:

$$M = \begin{bmatrix} m_x & 0 \\ 0 & m_y \end{bmatrix}, \quad C = \begin{bmatrix} c_x & 0 \\ 0 & c_y \end{bmatrix}, \quad K = \begin{bmatrix} k_x & 0 \\ 0 & k_y \end{bmatrix} \tag{2}$$

Also, $\mathbf{x}(t) = [x\ y]^T$ are the tool displacements along x-axis and y-axis, $\mathbf{F(t)} = [F_x\ F_y]^T$ are the cutting forces. Representing eqn. (1) along x-axis and y-axis:

$$\begin{bmatrix} m_x & 0 \\ 0 & m_y \end{bmatrix}\begin{bmatrix} \ddot{x} \\ \ddot{y} \end{bmatrix} + \begin{bmatrix} c_x & 0 \\ 0 & c_y \end{bmatrix}\begin{bmatrix} \dot{x} \\ \dot{y} \end{bmatrix} + \begin{bmatrix} k_x & 0 \\ 0 & k_y \end{bmatrix}\begin{bmatrix} x \\ y \end{bmatrix} = \begin{bmatrix} F_x \\ F_y \end{bmatrix} \tag{3}$$

which implies:

$$\begin{aligned} [c]cm_x\ddot{x} + c_x\dot{x} + k_x x &= F_x \\ m_y\ddot{y} + c_y\dot{y} + k_y y &= F_y \end{aligned} \tag{4}$$

Tables (2-3) summarize the used variables in this article.

A. CUTTING FORCE DYNAMICS CONSIDERING NONLINEARITIES

It is very important to illustrate the dynamics of the cutting forces [3], [36] are shown in Fig. 2.

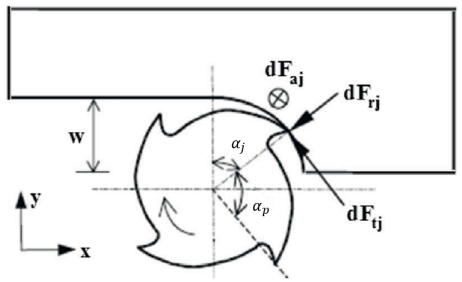

FIGURE 2. Dynamics of milling process [3], [36] .

The immersion angle α_j is computed in clockwise from the y-axis. The axial depth of cut z and the radial depth of cut w are assumed to be constant. Considering that the bottom end of one flute as the reference immersion angle and the bottom end point of the other flutes illustrated at the angles as:

$$\alpha_j = \alpha + j\alpha_p \quad \alpha_p = \frac{2\pi}{n} \quad j = 0, 1, 2, \ldots (N-1) \tag{5}$$

where α_p is the cutter pitch angle and n is the number of cutter teeth. Considering the lag angle at an arbitrary axial depth cut of z, the immersion angle of flute j is illustrated as [2]:

$$\alpha_j(z) = \alpha + j\alpha_p - \left(\frac{2z}{D}\right)\tan\beta \tag{6}$$

where β, and D, are the helix angle and the diameter of the cutter for and $j = 0, 1, \ldots (N-1)$. The cutting forces in

TABLE 2. Variable definitions.

Variable	Definition
$a_{i,x}, a_{i,y}$	Relative accelerations tool along x/y
$\tilde{A}$	Fuzzy set
C	Damping
c_x, c_y	Damping along x-axis and y-axis
d_{cx}, d_{cy}	Damper forces along x-axis and y-axis
D	Diameter of the cutter
f_l^z, f_r^z	Left firing strength, right firing strength
f_d	Damper force
F_x, F_y	Cutting forces along x-axis and y-axis
$\tilde{F}_1^l, ..., \tilde{F}_n^l$	Fuzzy sets
$\tilde{H}_1^l, ..., \tilde{H}_n^l$	Fuzzy sets
$\ddot{g}_i$	Damper acceleration
$G_{\tilde{A}}(x,u)$	Membership function
$G_{\tilde{A}}^{up}(x)$	Upper membership functions
$G_{\tilde{A}}^{lo}(x)$	Lower membership functions
$h(\alpha_j)$	Variable tool chip thickness
J_x	Primary membership
K	Stiffness
k_x, k_y	Stiffness along x-axis and y-axis
M	Total mass
m_x, m_y	Mass along x-axis and y-axis
m_d	Damper mass
n	Number of cutter teeth
Q	Total rules
$r(\alpha_j)$	Unit step function
u_{cx}, u_{cy}	Control signal along x-axis and y-axis
w	Radial depth of cut
w_{rk}, w_{lk}	Weighted functions
$\ddot{x}, \dot{x}, x$	Acceleration, velocity and position
$\ddot{x}_{i,x}, \ddot{x}_{i,y}$	Relative acceleration damper along x/y
y_{rk}, y_{lk}	Defuzzified crisp outputs
z	Axial depth of cut

x and y directions are represented as [11]:

$$\begin{aligned} F_x &= \sum_{j=0}^{N-1}\int_0^a dF_{x,j}(\alpha, z) \\ F_y &= \sum_{j=0}^{N-1}\int_0^a dF_{y,j}(\alpha, z) \end{aligned} \tag{7}$$

where $dF_{x,j}(\alpha, z)$ and $dF_{y,j}(\alpha, z)$ are the elemental differential forces corresponding to an infinitesimal element thickness dz of the j^{th} tool in x and y directions. The elemental forces are given by:

$$\begin{aligned} dF_{x,j}(\alpha, z) &= -dF_{t,j}\cos\alpha_j(z) - dF_{r,j}\sin\alpha_j(z) \\ dF_{y,j}(\alpha, z) &= +dF_{t,j}\sin\alpha_j(z) - dF_{r,j}\cos\alpha_j(z) \end{aligned} \tag{8}$$

The forces $dF_{x,j}(\alpha, z)$ and $dF_{y,j}(\alpha, z)$ are the nonlinear forces. Nonlinear modeling of milling process is of greater

TABLE 3. Greek variable definitions.

Variable	Definition
α_j	Angle of flute immersion angle
α_p	Cutter pitch angle
β	Helix angle of the cutter
α_{st}, α_{ex}	Start immersion and exit immersion
τ	Time delay
Ω	Spindle speed
$\xi_1, ..., \xi_{4,}$	Cutting force coefficients
$\delta_1, ..., \delta_4$	Cutting force coefficients
$\zeta_1, ..., \zeta_3$	Coeffs for half-immersion up-milling along x
$\eta_1, ..., \eta_3$	Coeffs for half-immersion up-milling along x
$\gamma_1, ..., \gamma_4$	Coeffs for half-immersion up-milling along x
$\ddot{\gamma}_i$	Tool acceleration
$\zeta_1^*, ..., \zeta_3^*$	Coeffs for half-immersion up-milling along y
$\eta_1^*, ...\eta_3^*$	Coeffs for half-immersion up-milling along y
$\gamma_1^*, ..., \gamma_4^*$	Coeffs for half-immersion up-milling along y
φ	Inclination angle

importance as it has greater role in stability analysis criteria. The cutting forces are illustrated as a third order polynomial function of cut chip thickness, [25]:

$$\begin{aligned} dF_{t,,j}(\alpha, z) &= [\xi_1 h_j^3(\alpha_j(z)) + \xi_2 h_j^2(\alpha_j(z)) \\ &\quad + \xi_3 h_j(\alpha_j(z)) + \xi_4] d(t, z) \\ dF_{r,,j}(\alpha, z) &= [\delta_1 h_j^3(\alpha_j(z)) + \delta_2 h_j^2(\alpha_j(z)) \\ &\quad + \delta_3 h_j(\alpha_j(z)) + \delta_4] d(t, z) \end{aligned} \tag{9}$$

In the existence of regenerative chatter, the variable total chip thickness is:

$$h(\alpha_j) = \left[\Delta x \sin\alpha_j + \Delta y \cos\alpha_j\right] r(\alpha_j) \tag{10}$$

where,

$$r(\alpha_j) = \left\{ \begin{array}{l} 1 \ \alpha_{st} < \alpha_j < \alpha_{ex} \\ 0 \ \alpha_{st} > \alpha_j \text{ or } \alpha_{ex} < \alpha_j \end{array} \right\} \tag{11}$$

also, $r(\alpha_j)$ is the unit step function validating whether the tooth is in or out of the cut, and it is stated in terms of start immersion α_{st} and exit immersion α_{ex}.

Again, $\Delta x = x(t) - x(t-\tau), \Delta y = y(t) - y(t-\tau), \tau = \frac{2\pi}{n\Omega}$, where τ is the time delay. $[x(t)\, y(t)]$ and $[x(t-\tau)\, y(t-\tau)]$ exhibits dynamic displacement of the cutter considering present and previous tool periods. Ω is the spindle speed in rad/s. According to [23], the nonlinear cutting forces along x-axis and y-axis which are in a closed form are given by:

$$\begin{aligned} F_x = +\frac{N}{2\pi}\{&\zeta_1 \Delta x^3 + \eta_1 \Delta y^3 + \zeta_2 \Delta x^2 \\ &+ \eta_2 \Delta y^2 + \zeta_3 \Delta x + \eta_3 \Delta y + 3\gamma_1 \Delta x^2 \Delta y \\ &+ 3\gamma_2 \Delta x \Delta y^2 + 2\gamma_3 \Delta x \Delta y + \gamma_4\} \end{aligned}$$

$$\begin{aligned} F_y = -\frac{N}{2\pi}\{&\zeta_1^* \Delta x^3 + \eta_1^* \Delta y^3 \\ &+ \zeta_2^* \Delta x^2 + \eta_2^* \Delta y^2 + \zeta_3^* \Delta x + \eta_3^* \Delta y \\ &+ 3\gamma_1^* \Delta x^2 \Delta y + 3\gamma_2^* \Delta x \Delta y^2 \\ &+ 2\gamma_3^* \Delta x \Delta y + \gamma_4^*\} \end{aligned} \tag{12}$$

Taking into account the start immersion angle as 0 and the exit angle as $\frac{\pi}{2}$ the coefficients for half-immersion up-milling are calculated as:

$$\begin{aligned} \zeta_1 &= \frac{1}{4}\left[\xi_1 + \frac{3}{4}\pi\delta_1\right], \quad \eta_1 = \frac{1}{4}\left[\delta_1 + \frac{3}{4}\pi\xi_1\right], \\ \zeta_2 &= \frac{1}{3}\left[\xi_2 + 2\delta_2\right], \eta_2 = \frac{1}{3}\left[\delta_2 + 2\xi_2\right], \\ \zeta_3 &= \frac{1}{2}\left[\xi_3 + \frac{1}{2}\pi\delta_3\right], \quad \eta_3 = \frac{1}{2}\left[\delta_3 + \frac{1}{2}\pi\xi_3\right], \\ \gamma_1 &= \frac{1}{4}\left[\delta_1 + \frac{1}{4}\pi\xi_1\right], \quad \gamma_2 = \frac{1}{4}\left[\xi_1 + \frac{1}{4}\pi\delta_1\right], \\ \gamma_3 &= \frac{1}{3}\left[\delta_2 + \xi_2\right], \quad \gamma_4 = \left[\xi_4 + \delta_4\right], \\ \zeta_1^* &= \frac{1}{4}\left[-\delta_1 + \frac{3}{4}\pi\xi_1\right], \quad \eta_1^* = \frac{1}{4}\left[\xi_1 - \frac{3}{4}\pi\delta_1\right], \\ \zeta_2^* &= , \frac{1}{3}\left[-\delta_2 + 2\xi_2\right], \quad \eta_2^* = \frac{1}{3}\left[\xi_2 - 2\delta_2\right], \\ \zeta_3^* &= \frac{1}{2}\left[-\delta_3 + \frac{1}{2}\pi\xi_3\right], \quad \eta_3^* = \frac{1}{2}\left[\xi_3 - \frac{1}{2}\pi\delta_3\right], \\ \gamma_1^* &= \frac{1}{4}\left[\xi_1 - \frac{1}{4}\pi\delta_1\right], \quad \gamma_2^* = \frac{1}{4}\left[-\delta_1 + \frac{1}{4}\pi\xi_1\right], \\ \gamma_3^* &= \frac{1}{3}\left[\xi_2 - \delta_2\right], \quad \gamma_4^* = \left[-\delta_4 + \xi_4\right] \end{aligned} \tag{13}$$

where $\xi_1, \xi_2, \ldots, \delta_1, \delta_2, \ldots$ are the cutting force coefficients.

B. ACTIVE CONTROL WITH ACTIVE VIBRATION DAMPER

To attenuate the tool chatter vibration caused by the external force, an *AVD* is installed on the top of the spindle, Fig. 3, where *AVD* is a linear servo actuator. The main action of the linear actuator is to converts the rotary motion of a servo into linear motion thus attenuating lateral vibration. The *AVD* is placed at the centre of mass making an inclination φ with the

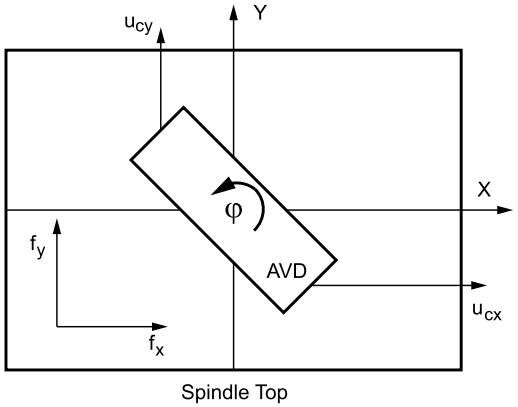

FIGURE 3. *AVD* **on Spindle Top.**

centre of mass. This methodology is been adopted to mitigate the problem of space during the placement of damper and also by making the arrangements cost effective by using one damper instead of two. The modeling equation of milling process with the control force $\mathbf{u_c}$ is:

$$M\ddot{\mathbf{x}}(t) + C\dot{\mathbf{x}}(t) + K\mathbf{x}(t) = \mathbf{F(t)} + \mathbf{u_c} - \mathbf{d_c} \tag{14}$$

where $\mathbf{u_c} = \begin{bmatrix} u_{cx} & u_{cy} \end{bmatrix}^T \in \Re^{2\times 1}$ are the control signals applied to the dampers along x-axis and y-axis, $\mathbf{d_c} = \begin{bmatrix} d_{cx} & d_{cy} \end{bmatrix} \in \Re^{2\times 1}$ are the damping and friction force vector of the damper along x-axis and y-axis. The closed-loop system, eqn. (1), along x and y component is:

$$\begin{aligned} m_x\ddot{x} + c_x\dot{x} + k_x x &= F_x + u_{cx} - d_{cx} \\ m_y\ddot{y} + c_y\dot{y} + k_y y &= F_y + u_{cy} - d_{cy} \end{aligned} \tag{15}$$

The damper force f_d is:

$$f_d = m_d(\ddot{g}_i + \ddot{\gamma}_i) \tag{16}$$

where m_d is the mass of the damper, $\ddot{g}_i$ is the acceleration of the damper, $\ddot{\gamma}_i$ is the acceleration of the tool relative to the damper, $\ddot{\gamma}_i = \sqrt{a_{i,x} + a_{i,y}}$, where $a_{i,x}$ and $a_{i,y}$ are the relative accelerations of the tool along x and y directions respectively, f_d should be separated into x and y directions as:

$$\begin{aligned} u_{i,x} &= f_d \cos\varphi = m_d(\ddot{g}_i \cos\varphi + a_{i,x}) \\ u_{i,y} &= f_d \sin\varphi = m_d(\ddot{g}_i \sin\varphi + a_{i,y}) \\ \ddot{\gamma}_i &= \frac{a_{i,x}}{\cos\varphi} = \frac{a_{i,y}}{\sin\varphi} \\ \ddot{x}_{i,x} &= a_{i,x} + \ddot{g}_i \cos\varphi, \qquad \ddot{x}_{i,y} = a_{i,y} + \ddot{g}_i \sin\varphi \end{aligned} \tag{17}$$

where φ is the angle of the damper along x-axis, $\ddot{x}_{i,x}$ and $\ddot{x}_{i,y}$ are the relative acceleration of the damper along x and y directions:

$$f_d = m_d\left(\ddot{g}_i + \frac{a_{i,x}}{\cos\varphi}\right) = m_d\left(\ddot{g}_i + \frac{a_{i,y}}{\sin\varphi}\right) \tag{18}$$

The control force of the damper along x and y directions are defined as $\mathbf{u_c} = \begin{bmatrix} u_{cx} & u_{cy} \end{bmatrix}^T$:

$$\mathbf{u_c} = m_{di}\begin{bmatrix} \ddot{x}_{i,x} & \ddot{x}_{i,y} \end{bmatrix}^T \tag{19}$$

Considering the friction of the damper:

$$\begin{aligned} d_{cx} &= fr_{i,x} = c\dot{x}_{i,x} + \epsilon m_d g \tanh\left[\beta\dot{x}_{i,x}\right] \\ d_{cy} &= fr_{i,y} = c\dot{x}_{i,y} + \epsilon m_d g \tanh\left[\beta\dot{x}_{i,y}\right] \end{aligned} \tag{20}$$

where c, β and ϵ are the damping coefficients of the *Coulomb* friction [28]. Considering eguations(15) and (20) the closed-loop system with control along x and y directions is:

$$\begin{aligned} m_x\ddot{x} + c_x\dot{x} + k_x x &= F_x + u_{cx} - c\dot{x}_{i,x} - \epsilon m_d g \tanh\left[\beta\dot{x}_{i,x}\right] \\ m_y\ddot{y} + c_y\dot{y} + k_y y &= F_y + u_{cy} - c\dot{x}_{i,y} - \epsilon m_d g \tanh\left[\beta\dot{x}_{i,y}\right] \end{aligned} \tag{21}$$

The terms

$$\begin{aligned} f_x &= c\dot{x}_{i,x} + \epsilon m_d g \tanh\left[\beta\dot{x}_{i,x}\right] - F_x \\ f_y &= c\dot{x}_{i,y} + \epsilon m_d g \tanh\left[\beta\dot{x}_{i,y}\right] - F_y \end{aligned} \tag{22}$$

are nonlinear, where $\mathbf{F} = [f_x f_y]^T$ then, an intelligent technique has to be applied to compensate the nonlinearities involved.

III. TYPE-2 FUZZY COMPENSATION TECHNIQUE

An effective means of compensating nonlinearities have been suggested. The main five components of a Type-2 *Fuzzy Logic System* (*FLS*) Fig. 4, are categorized as fuzzifier, rule base, Fuzzy inference engine, type-reducer and defuzzifier. A membership function validates a Type-2 Fuzzy set in which the membership value or grade associated to each element of this set is considered to be a Fuzzy set in the interval [0 1], instead of a crisp value. The membership functions of Type-2 Fuzzy sets are incorporated with three dimensional functions which is due to the (*FoU*) that supports Type-2 *FLS* with additional *DoF*. The advantage of Type-2 Fuzzy sets over the Type-1 counterparts is that the Type-2 can deal easily more patterns of uncertainties having higher magnitudes and using a smaller rule base. A Type-2 Fuzzy set is denoted by $\tilde{A}$ and it is characterized using a Type-2 membership function $G_{\tilde{A}}(x,u)$, where $x \epsilon X$ and $u \epsilon J_x \subseteq [0\ 1]$, i.e. [16], [30]:

$$\tilde{A} = \{(x,u), G_{\tilde{A}}(x,u) \mid \forall\, x\epsilon X, \forall\, u\epsilon J_x \subseteq [0\ 1]\} \tag{23}$$

also, $0 \leqslant G_{\tilde{A}}(x,u) \leqslant 1$. Taking into consideration a continuos universe of discourse, $\tilde{A}$ can be expressed as

$$\tilde{A} = \int_{x\epsilon X}\int_{u\epsilon J_x} G_{\tilde{A}}(x,u)/(x,u), \quad J_x \subseteq [0\ 1] \tag{24}$$

where J_x is stated to be as the primary membership of x. The discrete Fuzzy sets are illustrated by the symbol $\sum$ instead of using $\int$ associated with Type-1 Fuzzy logic. The secondary membership function which is par with $x = \acute{x}$, considering $\acute{x}$ ϵ X is illustrated as a Type-1 membership function stated by $G_{\tilde{A}}(x = \acute{x}, u), \forall\, u \epsilon J_x$. It is important to state that the *FoU* is considered to be the union of all primary memberships.

$$FoU(\tilde{A}) = U_{x\epsilon X} J_x \tag{25}$$

Consider $G^{up}_{\tilde{A}}(x)$ and $G^{lo}_{\tilde{A}}(x)$ to be the upper and lower membership functions which are Type-1 that describes the upper and lower bounds respectively of the *FoU* having interval Type-2 membership function $G_{\tilde{A}}(x,u)$. Type-2 *FLS* resembles Type-1 *FLS* as the structure of rules in the Type-2 *FLS* as well as its inference engine are similar.

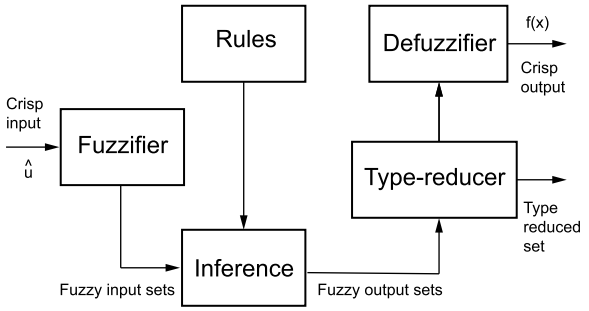

FIGURE 4. Block diagram of Type-2 *FLS*.

The feasibility and less complexity involved within Type-2 *FLS* is the main reason behind the formulation of interval Fuzzy sets, [16]. The methodology involved in the fuzzification stage is that the crisp input vector having n elements $x = (x_1, x_2, \ldots, x_n)^T$ in the universe of discourse $X_1 \times X_2 \times \ldots \times X_n$ is mapped into Type-2 Fuzzy sets [16]. The calculation of upper and lower membership functions are achieved for each point of the universe of discourse thus generating an interval Type-1 set $[f_l^{lo}\ f_l^{up}]$ taking into consideration each rule l, in this case:

$$[f_l^{lo}\ f_l^{up}] = [f_l^{lo}(\acute{x})\ f_l^{up}(\acute{x})] \tag{26}$$

where:

$$\begin{aligned} f_l^{lo}(\acute{x}) &= G^{lo}_{\tilde{F}_1^l}(\acute{x}_1) *, \ldots, * G^{lo}_{\tilde{F}_p^l}(\acute{x}_1) \\ f_l^{up}(\acute{x}) &= G^{up}_{\tilde{F}_1^l}(\acute{x}_1) *, \ldots, * G^{up}_{\tilde{F}_p^l}(\acute{x}_1) \end{aligned} \tag{27}$$

again $*$ denotes *t-norm* operator. The *IF-THEN* rules associated with Type-2 has got the similar structure as Type-1 counterpart. In this methodology, the antecedents and the consequents are demonstrated using interval Type-2 Fuzzy sets. Hence the l^{th} rule is [5]:

$$\begin{aligned} R^l :\ & IF\ (x_1\ is\ \tilde{F}_1^l)\ and\ (x_2\ is\ \tilde{F}_2^l)\ and, \ldots,\ and\ (x_n\ is\ \tilde{F}_n^l) \\ & THEN\ (y_1\ is \tilde{H}_1^l)\ and\ (y_2\ is\ \tilde{H}_2^l)\ and, \ldots,\ and\ (y_m\ is\ \tilde{H}_n^l) \end{aligned} \tag{28}$$

where $\tilde{F}_1^l, \tilde{F}_2^l, \ldots, \tilde{F}_n^l$ and $\tilde{H}_1^l, \tilde{H}_2^l, \ldots, \tilde{H}_n^l$ represents Fuzzy sets.

A Type-2 Fuzzy inference engine provides a mapping from the input Type-2 Fuzzy sets to the output ones. Each rule l in the knowledge base is interpreted as a Type-2 Fuzzy implication that, when aggregated with the fuzzified inputs, infers a Type-2 Fuzzy set $\tilde{O}^l$ such that:

$$G_{\tilde{O}^l}(y) = \sqcup_{x \epsilon X}[G_{\tilde{A}}(x) \sqcap G_{R^l}(x, y)] \tag{29}$$

The modified and extended from of Type-1 defuzzification methods is termed as Type-reduction method. A Type-2 output Fuzzy set is converted to a Type-1 Fuzzy set by implementing this methodology which is stated as Type-reduced set. The centroid of the t^{th} output Fuzzy set y_k^t which signifies Type-1 interval set and it is extracted using its left and right most points, y_{lk}^t and y_{rk}^t respectively, and it is demonstrated as [16]:

$$y_k^t = [y_{lk}^t\ y_{rk}^t] = y(\theta_1, \ldots, \theta_i) = \frac{\sum_{i=1}^I y_i \theta_i}{\sum_{i=1}^I \theta_i} \tag{30}$$

The application of the centroid method as well as utilizing the center-of-sets type reduction, the Type-2 Fuzzy sets can be reduced to an interval Type-1 Fuzzy set $[y_{lk}^z\ y_{rk}^z]$ considering each rule z. The deduced interval Type-1 Fuzzy set is:

$$y_{lk} = \frac{\sum_{z=1}^L f_l^z y_{lk}^z}{\sum_{z=1}^L f_l^z},\ y_{rk} = \frac{\sum_{z=1}^L f_r^z y_{rk}^z}{\sum_{z=1}^L f_r^z} \tag{31}$$

where $f_l^z\ f_r^z$ are the firing strengths associated with y_{lk}^z and y_{rk}^z of rule i. This operation is conducted to minimize y_{lk}^z and maximize y_{rk}^z. Also, y_{lk} and y_{rk} can be expressed numerically as:

$$y_{rk} = \frac{\sum_{e=1}^R f^{lo\_e} y_{rk}^e + \sum_{d=L+1}^Q f^{up\_d} y_{rk}^d}{\sum_{e=1}^R f^{lo\_e} + \sum_{d=R+1}^Q f^{up\_d}} \tag{32}$$

If Q is the total number of rules, then Q iterations are sufficient for the convergence of both procedures:

$$\begin{aligned} y_{lk} &= \sum_{e=1}^L q_{lk}^{lo\_e} y_{lk} + \sum_{d=L+1}^Q q^{up\_d} y_{lk} \\ &= [Q_{lk}^{lo}\ Q_{lk}^{up}] \begin{bmatrix} y_{lk}^{lo} \\ y_{lk}^{up} \end{bmatrix} = \xi_{lk}^T \ominus_{lk} \end{aligned} \tag{33}$$

where $q_{lk}^{lo\_e} = f^{lo\_e}/V_{lk}, q^{up\_d} = f^{up\_d}/V_{lk}$ and $V_{lk} = (\sum_{e=1}^L f^{lo\_e} + \sum_{d=L+1}^Q f^{up\_d})$. Also, $\xi_{lk}^T = [Q_{lk}^{lo}\ Q_{lk}^{up}]$ and $\ominus_{lk}^T = [y_{lk}^{lo}\ y_{lk}^{up}]$

$$\begin{aligned} y_{rk} &= \sum_{e=1}^R q^{lo\_e} y_{rk} + \sum_{d=R+1}^Q q^{up\_d} y_{rk} \\ &= [Q_{rk}^{lo}\ Q_{rk}^{up}] \begin{bmatrix} y_{rk}^{lo} \\ y_{rk}^{up} \end{bmatrix} = \xi_{rk}^T \ominus_{rk} \end{aligned} \tag{34}$$

where $q_{rk}^{lo\_e} = f^{lo\_e}/V_{rk}, q^{up\_d} = f^{up\_d}/V_{rk}$ and $V_{rk} = (\sum_{e=1}^R f^{lo\_e} + \sum_{d=R+1}^Q f^{up\_d})$

Initially the Type-reduced set is extracted using its left most and right most points y_{lk} and y_{rk}. Then, it is defuzzified by the application of interval set average formula for the determination of crisp output. Hence, the defuzzified crisp output considering each output k is defined as [18] :

$$\begin{aligned} y(x) &= \frac{y_{rk} + y_{lk}}{2} = \frac{1}{2}(\xi_{rk}^T \ominus_{rk} + \xi_{lk}^T \ominus_{lk}) \\ &= \frac{1}{2}[\xi_{rk}^T\ \xi_{lk}^T] \begin{bmatrix} \ominus_{rk} \\ \ominus_{lk} \end{bmatrix} = \xi^T \ominus \end{aligned} \tag{35}$$

where $\xi^T = \frac{1}{2}[\xi_{rk}^T\ \xi_{lk}^T]$ and $\ominus^T = [\ominus_{rk}^T\ \ominus_{lk}^T]$. Based on the aforementioned concept, by singleton fuzzifier, the j^{th} output of the Fuzzy logic system can be expressed as:

$$\begin{aligned} \hat{f}_k &= \frac{y_{rk} + y_{lk}}{2} \\ &= \frac{1}{2}[(\phi_{rk}^T(z) w_{rk}(z) + \phi_l^T(z) w_{lk}(z)] \end{aligned} \tag{36}$$

where $k = 1, 2$ w_{rk} is the point at which $\mu_{B_{rk}} = 1$, w_{lk} is the point at which $\mu_{B_{lk}} = 1$, $z = [x\ y\ \dot{x}\ \dot{y}]^T$, in matrix form, the estimation of the uncertainty $\mathbf{F}$ is:

$$\hat{\mathbf{F}} = \frac{1}{2}\left[\Phi_r^T(z) W_r(z) + \Phi_l^T(z) W_l(z)\right] \tag{37}$$

where $\hat{F} = \left[\hat{f}_1\ \hat{f}_2\right] = [\hat{f}_x\ \hat{f}_y]^T$. Representing the estimation of uncertainty along x and y directions, where $z_x = [x\ \dot{x}]$ and $z_y = [y\ \dot{y}]$:

$$\begin{aligned} \hat{f}_x &= \frac{1}{2}\left[\theta_r^T(z_x) w_r(z_x) + \theta_l^T(z_x) w_l(z_x)\right] \\ \hat{f}_y &= \frac{1}{2}\left[\theta_r^T(z_y) w_r(z_y) + \theta_l^T(z_y) w_l(z_y)\right] \end{aligned} \tag{38}$$

IV. PD CONTROLLER WITH TYPE-2 FUZZY COMPENSATION

The *PD* controller is the simplest algorithm that provides high robustness into the classical controllers domain. The pattern of *PD* controller, where K_p and K_d are positive-definite constant matrices, which correspond to the proportional and derivative gains given by (39). The design of the controller is based on the suitable gain selection K_p and K_d such that the closed-loop system is stable and good performance are achieved. For the chatter control, the gains of *PD* are: $K_P = diag\left(K_{px}, K_{py}\right) \in \Re^{2x2}$, and $K_d = diag\left(K_{dx}, K_{dy}\right) \in \Re^{2x2}$.

$$\mathbf{u} = -K_p\mathbf{e} - K_d\dot{\mathbf{e}} \tag{39}$$

where $\mathbf{e} = \mathbf{x} - \mathbf{x}^d$ is the error, $\mathbf{x}^d$ is the expected tool vibration. For vibration control, $\mathbf{x}^d = 0$, then:

$$\mathbf{u} = -K_p\mathbf{x} - K_d\dot{\mathbf{x}} \tag{40}$$

Considering the inputs for x and y directions:

$$\begin{aligned} u_{cx} &= -K_{px}x - K_{dx}\dot{x} \\ u_{cy} &= -K_{py}y - K_{dy}\dot{y} \end{aligned} \tag{41}$$

PD controller with Type-2 Fuzzy compensation along $x-$direction is:

$$u_{cx} = -K_{px}x - K_{dx}\dot{x} - \frac{1}{2}[\theta_r^T(z_x)w_r(z_x) + \theta_l^T(z_x)w_l(z_x)] \tag{42}$$

Also, along $y-$direction, *PD* control with Type-2 Fuzzy compensation is:

$$u_{cy} = -K_{py}y - K_{dy}\dot{y} - \frac{1}{2}[\theta_r^T(z_y)w_r(z_y) + \theta_l^T(z_y)w_l(z_y)] \tag{43}$$

Using equations (21), (22) and (42), the closed-loop system with Type-2 Fuzzy compensation and *PD* controller along $x-$direction is:

$$\begin{aligned} m_x\ddot{x} + c_x\dot{x} + k_xx + f_x &= -K_{px}x - K_{dx}\dot{x} \\ &\quad - \frac{1}{2}\left[\theta_r^T(z_x)w_r(z_x) + \theta_l^T(z_x)w_l(z_x)\right] \end{aligned} \tag{44}$$

For the y-direction, the closed-loop system is:

$$\begin{aligned} m_y\ddot{y} + c_y\dot{y} + k_yy + f_y &= -K_{py}y - K_{dy}\dot{y} \\ &\quad - \frac{1}{2}\left[\theta_r^T(z_y)w_r(z_y) + \theta_l^T(z_y)w_l(z_y)\right] \end{aligned} \tag{45}$$

Since the pattern of two components x and y exhibits same form, the analysis will be carried out considering only x-direction. Let $K_{px}x + K_{dx}\dot{x} = L_x(\dot{x} + \omega_x x)$, also $K_{px}x = L_x\omega_x$ and $K_{dx} = L_x$, where ω_x is a positive definite matrix, L_x is a positive variable. Equation (44) becomes:

$$\begin{aligned} &m_x\ddot{x} + c_x\dot{x} + k_xx + f_x \\ &\quad = -L_x(\dot{x} + \omega_x x) \\ &\qquad - \frac{1}{2}\left[\theta_r^T(z_x)w_r(z_x) + \theta_l^T(z_x)w_l(z_x)\right] \end{aligned} \tag{46}$$

$$\begin{aligned} &m_x(\ddot{x} + \omega_x\dot{x}) \\ &\quad = -c_x\dot{x} - k_xx - f_x \\ &\qquad - L_x(\dot{x} + \omega_x x) - \frac{1}{2}[\theta_r^T(z_x)w_r(z_x) \\ &\qquad + \theta_l^T(z_x)w_l(z_x)] = -c_x\dot{x} + c_x\omega_x x - c_x\omega_x x \\ &\qquad - (\omega_x\omega_x^{-1})k_xx + \omega_x^{-1}k_x\dot{x} - \omega_x^{-1}k_x\dot{x} - f_x \\ &\qquad - L_x(\dot{x} + \omega_x x) - \frac{1}{2}[\theta_r^T(z_x)w_r(z_x) \\ &\qquad + \theta_l^T(z_x)w_l(z_x)] + m_x\omega_x\dot{x} \\ &\quad = -L_x(\dot{x} + \omega_x x) - c_x(\dot{x} + \omega_x x) \\ &\qquad - \omega_x^{-1}k_x(\dot{x} + \omega_x x) \\ &\qquad - \frac{1}{2}\left[\theta_r^T(z_x)w_r(z_x) + \theta_l^T(z_x)w_l(z_x)\right] \\ &\qquad + [(m_x\omega_x + k_x\omega_x^{-1})\dot{x} + c_x\omega_x x - f_x] \end{aligned} \tag{47}$$

According to the Theorem Stone-Weierstrass, [20], the general nonlinear smooth function can be illustrated as:

$$\begin{aligned} &(m_x\omega_x + k_x\omega_x^{-1})\dot{x} + c_x\omega_x x - f_x \\ &\qquad = \frac{1}{2}\left[\theta_r^T(z_x)w_r^*(z_x) + \theta_l^T(z_x)w_l^*(z_x)\right] + e_x \end{aligned} \tag{48}$$

where e_x is the modeling error, $w_r^*(z_x)$ and $w_l^*(z_x)$ are the unknown optimal weights. The boundary conditions satisfy the next inequality, where ω_e is a positive definite matrix:

$$e_x^T\omega_{ex}^{-1}e_x \le \tilde{e}_x \tag{49}$$

Theorem 1: Suppose the closed-loop system of a milling process represented by eqn. (14) is controlled by Type-2 Fuzzy PD controllers mentioned by eguations (42) and (43) where the gain satisfies

$$K_{dx} > \omega_{fx}, \quad K_{dy} > \omega_{fy} \tag{50}$$

and if the updated laws of the Fuzzy systems are:

$$\begin{aligned} \frac{d}{dt}\tilde{w}_r(z_x) &= -\rho_r[(\dot{x} + \omega_x x)^T\theta_r(z_x)]^T \\ \frac{d}{dt}\tilde{w}_l(z_x) &= -\rho_l[(\dot{x} + \omega_x x)^T\theta_l(z_x)]^T \\ \frac{d}{dt}\tilde{w}_r(z_y) &= -\rho_r[(\dot{y} + \omega_y y)^T\theta_r(z_y)]^T \\ \frac{d}{dt}\tilde{w}_l(z_y) &= -\rho_l[(\dot{y} + \omega_y y)^T\theta_l(z_y)]^T \end{aligned} \tag{51}$$

then, the states of the closed-loop systems eguations (44) and (45) are bounded and stability is assured provided

$$\begin{aligned} \lim_{T\to 0}\frac{1}{T}\int_0^T &[\parallel (\dot{x} + \omega_x x)^T \parallel^2_{k_{ax}+k_{bx}} \\ &+ \parallel (\dot{y} + \omega_y y)^T \parallel^2_{k_{ay}+k_{by}}] \le \tilde{e}_x + \tilde{e}_y \end{aligned} \tag{52}$$

where $e_x^T\omega_{ex}^{-1}e_x \le \tilde{e}_x$, $e_y^T\omega_{ey}^{-1}e_y \le \tilde{e}_y$, $\omega_x^{-1}k_x - \omega_{gx} > 0$, $\omega_y^{-1}k_y - \omega_{gy} > 0$.

Proof: Consider Lyapunov candidate V_x along $x-$component

$$\begin{aligned} V_x &= \frac{1}{2}(\dot{x} + \omega_x x)^T m_x(\dot{x} + \omega_x x) \\ &\quad + \frac{1}{4\rho_r}\pi_1[\tilde{w}_r^T(z_x)\tilde{w}_r(z_x)] + \frac{1}{4\rho_l}\pi_2[\tilde{w}_l^T(z_x)\tilde{w}_l(z_x)] \end{aligned} \tag{53}$$

Since m_x is positive definite matrices and $\rho_r > 0$, $\rho_l > 0$, $V_x \geq 0$. Also,

$$\tilde{w}_r(z_x) = w_r^*(z_x) - w_r(z_x)$$
$$\tilde{w}_l(z_x) = w_l^*(z_x) - w_l(z_x) \quad (54)$$

The derivative of eqn. (53) gives:

$$\dot{V}_x = (\dot{x} + \omega_x x)^T m_x(\ddot{x} + \omega_x \dot{x}) + \frac{1}{2\rho_r}\pi_1[\tilde{w}_r^T(z_x)\frac{d}{dt}\tilde{w}_r(z_x)] + \frac{1}{2\rho_l}\pi_2[\tilde{w}_l^T(z_x)\frac{d}{dt}\tilde{w}_l(z_x)] \quad (55)$$

Using equations (47) and (48) in eqn. (55)

$$\begin{aligned}\dot{V}_x &= (\dot{x} + \omega_x x)^T\{L_x(\dot{x} + \omega_x x) - c_x(\dot{x} + \omega_x x) - \omega_x^{-1}k_x(\dot{x} + \omega_x x) \\ &\quad - \frac{1}{2}\left[\theta_r^T(z_x)w_r(z_x) + \theta_l^T(z_x)w_l(z_x)\right]\} \\ &\quad + \{\frac{1}{2}\left[\theta_r^T(z_x)w_r^*(z_x) + \theta_l^T(z_x)w_l^*(z_x)\right] + e_x\} \\ &\quad + \frac{1}{2\rho_r}\pi_1[\tilde{w}_r^T(z_x)\frac{d}{dt}\tilde{w}_r(z_x)] + \frac{1}{2\rho_l}\pi_2[\tilde{w}_l^T(z_x)\frac{d}{dt}\tilde{w}_l(z_x)] \\ &= -(\dot{x} + \omega_x x)^T[L_x(\dot{x} + \omega_x x) + c_x(\dot{x} + \omega_x x) + \omega_x^{-1}k_x(\dot{x} + \omega_x x)] \\ &\quad + (\dot{x} + \omega_x x)^T[\frac{1}{2}\theta_r^T(z_x)\{w_r^*(z_x) - w_r(z_x)\}] \\ &\quad + (\dot{x} + \omega_x x)^T[\frac{1}{2}\theta_l^T(z_x)w_l^*(z_x)\{w_l^*(z_x) - w_l(z_x)\}] + (\dot{x} + \omega_x x)^T e_x \\ &\quad + \frac{1}{2\rho_r}\pi_1[\tilde{w}_r^T(z_x)\frac{d}{dt}\tilde{w}_r(z_x)] + \frac{1}{2\rho_l}\pi_2[\tilde{w}_l^T(z_x)\frac{d}{dt}\tilde{w}_l(z_x)] \quad (56)\end{aligned}$$

Consider the updated law for the Fuzzy system as follows:

$$\frac{d}{dt}\tilde{w}_r(z_x) = -\rho_r[(\dot{x} + \omega_x x)^T\theta_r(z_x)]^T$$
$$\frac{d}{dt}\tilde{w}_l(z_x) = -\rho_l[(\dot{x} + \omega_x x)^T\theta_l(z_x)]^T \quad (57)$$

Combining equations (54) and (57) in eqn. (56)

$$\begin{aligned}\dot{V}_x &= -(\dot{x} + \omega_x x)^T[L_x(\dot{x} + \omega_x x) + c_x(\dot{x} + \omega_x x) + \omega_x^{-1}k_x(\dot{x} + \omega_x x)] + (\dot{x} + \omega_x x)^T e_x \\ &\quad + (\dot{x} + \omega_x x)^T[\frac{1}{2}\theta_r^T(z_x)\{\tilde{w}_r(z_x) - \tilde{w}_r(z_x)\}] \\ &\quad + (\dot{x} + \omega_x x)^T[\frac{1}{2}\theta_l^T(z_x)\{\tilde{w}_l(z_x) - \tilde{w}_l(z_x)\}] \\ &= -(\dot{x} + \omega_x x)^T[L_x(\dot{x} + \omega_x x) + c_x(\dot{x} + \omega_x x) + \omega_x^{-1}k_x(\dot{x} + \omega_x x)] + (\dot{x} + \omega_x x)^T e_x \quad (58)\end{aligned}$$

The property of matrix inequality gives:

$$A^T B + B^T A = A^T \omega A + B^T \omega^{-1} B \quad (59)$$

The relation eqn. (59) is valid for all $A, B \in R^n$, $\omega = \omega^T > 0$, then:

$$(\dot{x} + \omega_x x)^T e_x \leq (\dot{x} + \omega_x x)^T \omega_{ex}(\dot{x} + \omega_x x) + e_x^T \omega_{ex}^{-1} e_x \quad (60)$$

Since the term $e_x^T \omega_{ex}^{-1} e_x$ is bounded by the relation eqn. (49), and also $\omega_{ex} > 0$ and let $L_x > \omega_{fx} > 0$, $\omega_x^{-1}k_x > \omega_{gx} > 0$. From eqn. (58):

$$\begin{aligned}\dot{V}_x &\leq -(\dot{x} + \omega_x x)^T[(L_x + c_x - \omega_{fx}) + (\omega_x^{-1}k_x - \omega_{gx})](\dot{x} + \omega_x x) + \tilde{e}_x \\ &\leq - \parallel (\dot{x} + \omega_x x)^T \parallel^2 [(L_x + c_x - \omega_{fx}) + (\omega_x^{-1}k_x - \omega_{gx})] + \tilde{e}_x \quad (61)\end{aligned}$$

Let $L_x + c_x - \omega_{fx} = k_{ax}$ and $\omega_x^{-1}k_x - \omega_{gx} = k_{bx}$, then using eqn. (61):

$$\dot{V}_x \leq - \parallel (\dot{x} + \omega_x x)^T \parallel^2_{k_{ax}+k_{bx}} + \tilde{e}_x \quad (62)$$

Considering the concept presented by [32], $(\dot{x} + \omega_x x)$ is bounded when $e_y^T \omega_{ey}^{-1} e_y \leq \tilde{e}_y$ and let $L_x + c_x - \omega_{fx} > 0$, $\omega_x^{-1}k_x - \omega_{gx} > 0$, therefore:

$$\int_0^T \dot{V}_x \leq -\int_0^T \parallel (\dot{x} + \omega_x x)^T \parallel^2_{k_{ax}+k_{bx}} dt + \tilde{e}_x T$$
$$\int_0^T \parallel (\dot{x} + \omega_x x)^T \parallel^2_{k_{ax}+k_{bx}} dt \leq V_0 - V_T + \tilde{e}_x T$$
$$Lim_{T\to 0}\frac{1}{T}\int_0^T \parallel (\dot{x} + \omega_x x)^T \parallel^2_{k_{ax}+k_{bx}} \leq \tilde{e}_x \quad (63)$$

Considering a similar analysis along $y-$component, $(\dot{y}+\omega_x y)$ is bounded when e_y is bounded by $\tilde{e}_y$ and $L_y + c_y - \omega_{fy} > 0$, $\omega_y^{-1}k_y - \omega_{gy} > 0$. Hence,

$$Lim_{T\to 0}\frac{1}{T}\int_0^T \parallel (\dot{y} + \omega_y y)^T \parallel^2_{k_{ay}+k_{by}} \leq \tilde{e}_y \quad (64)$$

where $k_{ay} = L_y + c_y - \omega_{fy}$ and $k_{by} = \omega_y^{-1}k_y - \omega_{gy}$. Adding equations (63) and (64), the boundary conditions of $(\dot{x}+\omega_x x)$ and $(\dot{y} + \omega_y y)$ are achieved by:

$$\lim_{T\to 0}\frac{1}{T}\int_0^T [\parallel (\dot{x} + \omega_x x)^T \parallel^2_{k_{ax}+k_{bx}} + \parallel (\dot{y} + \omega_y y)^T \parallel^2_{k_{ay}+k_{by}}] \leq \tilde{e}_x + \tilde{e}_y \quad (65)$$

■

Remark 1: The potential ability of adaptive Fuzzy compensation eqn. (46) is that it does not be worry about the big compensation error existing in eqn. (48), which is an outcome of selecting a poor membership function. The gradient algorithms eqn. (57) validates the updates of the membership functions $w_r(z_x)$ and $w_l(z_x)$ in such a way that the system states are bounded as well as error approaches towards zero. Theorem 1 guarantees that the updating algorithms are stable. There is a tendency of regulation error to become small with the increase of the derivative gain. But the large derivative gain results in slow transient performance. The error converges to zero under the condition that derivative gain tends

to infinity [15]. It is utter necessary to increase the derivative gain K_d to decrease the steady-state errors caused by these uncertainties.

V. PID CONTROLLER WITH TYPE-2 FUZZY COMPENSATION

PID controllers use feedback strategy and have three actions: *P*-action is introduced for increasing the speed of response, *D*-action is introduced for damping purposes and *I*-action is introduced for obtaining a desired steady-state response [7]. The control law involving *PID* is given by:

$$\mathbf{u} = -K_p(\mathbf{e}) - K_i \int_0^t (\mathbf{e}) d\tau - K_d(\dot{\mathbf{e}}) \tag{66}$$

where K_p, K_i and K_d are positive definite, K_i is the integral gain. For vibration control, $\mathbf{x}^d = 0$, then using eqn. (66):

$$\mathbf{u} = -K_p\mathbf{x} - K_i \int_0^t \mathbf{x} d\tau - K_d\dot{\mathbf{x}} \tag{67}$$

PID controller with Type-2 Fuzzy compensation along $x-$direction is:

$$u_{cx} = -K_{px}x - K_{ix}\int_0^t x d\tau - K_{dx}\dot{x} - \frac{1}{2}\left[\theta_r^T(z_x)w_r(z_x) + \theta_l^T(z_x)w_l(z_x)\right] \tag{68}$$

Also, along $y-$direction, *PID* controller with Type-2 Fuzzy compensation is:

$$u_{cy} = -K_{py}y - K_{iy}\int_0^t x d\tau - K_{dy}\dot{y} - \frac{1}{2}\left[\theta_r^T(z_y)w_r(z_y) + \theta_l^T(z_y)w_l(z_y)\right] \tag{69}$$

Using equations (21), (22) and (68), the closed-loop system with Type-2 Fuzzy compensation and *PID* controller along $x-$direction is:

$$\begin{aligned} m_x\ddot{x} + c_x\dot{x} + k_x x + f_x &= -K_{px}x - K_{ix}\int_0^t x d\tau - K_{dx}\dot{x} \\ &\quad - \frac{1}{2}[\theta_r^T(z_x)w_r(z_x) + \theta_l^T(z_x)w_l(z_x)] \end{aligned} \tag{70}$$

Considering the y-direction, the closed-loop system becomes:

$$\begin{aligned} m_y\ddot{y} + c_y\dot{y} + k_y y + f_y &= -K_{py}y - K_{iy}\int_0^t x d\tau - K_{dy}\dot{y} - K_{dy}\dot{y} \\ &\quad - \frac{1}{2}\left[\theta_r^T(z_y)w_r(z_y) + \theta_l^T(z_y)w_l(z_y)\right] \end{aligned} \tag{71}$$

Since the pattern of two components x and y exhibits is similar, the analysis will be carried out considering x-direction only. Assume $K_{iy}\int_0^t x d\tau = \xi_x$, therefore from eqn. (68) it can be demonstrated:

$$\begin{aligned} \dot{x} &= -m_x(c_x\dot{x} + k_x x + f_x + K_{px}x + \xi_x \\ &\quad + K_{dx}\dot{x} + \frac{1}{2}\theta_r^T(z_x)w_r(z_x) + \frac{1}{2}\theta_l^T(z_x)w_l(z_x) \\ \dot{\xi}_x &= K_{ix}x \end{aligned} \tag{72}$$

From equations (72) it is clear that eqn. (70) origin is not at equilibrium and is $[x\ \dot{x}\ \xi_x] = \left[0\ 0\ \xi_x^*\right]$. To change the origin at equilibrium, $x = 0$, $\dot{x} = 0$, the equilibrium is $[0\ 0\ \rho_x(0,0)]$, so $\xi_x^* = \xi_x - \rho_x(0,0)$, ρ_x is unknown modeling error. The f_x will be estimated using Type-2 Fuzzy as:

$$f_x = \frac{1}{2}\theta_r^T(z_x)w_r^*(z_x) + \frac{1}{2}\theta_l^T(z_x)w_l^*(z_x) + \rho_x \tag{73}$$

Therefore using eqn. (73) in (70):

$$\begin{aligned} &m_x\ddot{x} + c_x\dot{x} + k_x x + \frac{1}{2}\theta_r^T(z_x)w_r^*(z_x) \\ &\quad + \frac{1}{2}\theta_l^T(z_x)w_l^*(z_x) + \rho_x \\ &= -K_{px}x - \xi_x + \rho_x(0,0) - K_{dx}\dot{x} \\ &\quad - \frac{1}{2}[\theta_r^T(z_x)w_r(z_x) + \theta_l^T(z_x)w_l(z_x)] \end{aligned} \tag{74}$$

The modeling error ρ_x is the function of two nonlinear forces: damper friction and cutting force. The lower bound of the modeling error is:

$$\begin{aligned} \int_0^t \rho_x &= \left(\int_0^t \rho_{dx}dx - \frac{1}{2}\int_0^t \theta_r^T(z_x)w_r(z_x) \right. \\ &\quad \left. - \frac{1}{2}\int_0^t \theta_l^T(z_x)w_l(z_x)\right) + \int_0^t \rho_{fx}dx \\ &= \rho_{1x} + \rho_{2x} \end{aligned} \tag{75}$$

The lower bound of $\rho_{1x} = \int_0^t \rho_{dx}dx - \frac{1}{2}\theta_r^T(z_y)w_r(z_y) - \frac{1}{2}\theta_l^T(z_y)w_l(z_y)$ is a first order continuous function satisfying *Lipschitz* condition:

$$\| \rho_{1x}(a) - \rho_{1x}(b) \| \leq k_{1x} \| a - b \| \tag{76}$$

where k_{1x} is a Lipschitz constant. The lower bound of damping uncertainties is $\int_0^t \rho_{dx}dx = -\bar{\rho}_{dx}$. Also, $\theta_r^T(z_x)$ and $\theta_l^T(z_x)$ are the Gaussian functions and so:

$$\begin{aligned} \frac{1}{2}\int_0^t \theta_r^T(z_x)w_r(z_x) &= \frac{w_r(z_x)}{4}\sqrt{\pi}\,\mathrm{erf}(z_x) \\ \frac{1}{2}\int_0^t \theta_l^T(z_x)w_l(z_x) &= \frac{w_l(z_x)}{4}\sqrt{\pi}\,\mathrm{erf}(z_x) \end{aligned} \tag{77}$$

so,

$$k_{1x} = -\bar{\rho}_{dx} - \frac{1}{4}\sqrt{\pi}\,\mathrm{erf}(z_x)\,[w_r(z_x) + w_l(z_x)] \tag{78}$$

Let the lower bound of the cutting force be $\bar{f}_{xl}(\Delta x, \Delta y)$, $\int_0^t \rho_{fx}dx = \bar{f}_{xl}(\Delta x, \Delta y)$, since the cutting force $F_x \epsilon$ $f_{xl}(\Delta x, \Delta y)$:

$$\bar{f}_{xl}(\Delta x, \Delta y) < k_{xl}(\Delta x, \Delta y) \tag{79}$$

Hence, $\bar{f}_{xl}(\Delta x, \Delta y)$ is bounded and $k_{xl}(\Delta x, \Delta y)$ is a constant value. The property of eigen values suggest that the positive definite matrix m_x satisfies the following conditions:

$$\begin{aligned} \| m_x \| &\geq \lambda_{\min}(m_x) > 0 \\ \bar{m} &\geq \lambda_{\max}(m_x) \geq \| m_x \| \end{aligned} \tag{80}$$

where $\lambda_{\max}(m_x)$ and $\lambda_{\min}(m_x)$ are the maximum and minimum eigenvalues of the matrix m_x. $\bar{m} > 0$ is the upper bound.

Theorem 2: Suppose the closed-loop system of a milling process represented by eqn. (14) is controlled by Type-2 Fuzzy PID controllers mentioned by equations (68) and (69), the closed-loop system will be asymptotically stable under the following gains conditions:

$$\begin{aligned}
\lambda_{\min}(K_{px}) &\geq [k_{1x} + k_{xl}(\Delta x, \Delta y) + \lambda_{\max}(c_x)] \\
&\quad + \frac{1}{\upsilon_x}[\lambda_{\max}(K_{ix}) - \lambda_{\min}(k_x) + \Gamma_{x\max}] \\
\lambda_{\min}(K_{dx}) &\geq \upsilon_x[\lambda_{\max}(m_x) + \lambda_{\max}(c_x)] \\
&\quad + [\Gamma_{x\max} - \lambda_{\min}(c_x)] \\
\lambda_{\max}(K_{ix}) &\leq \frac{\left(\lambda_{\min}(m_x))^{\frac{1}{2}}(\lambda_{\min}(K_{px})\right)^{\frac{3}{2}}}{6\sqrt{3}\lambda_{\max}(m_x)} \qquad (81) \\
\lambda_{\min}(K_{py}) &\geq [k_{1y} - k_{yl}(\Delta x, \Delta y) + \lambda_{\max}(c_y)] \\
&\quad + \frac{1}{\upsilon_y}[\lambda_{\max}(K_{iy}) - \lambda_{\min}(k_y) + \Gamma_{y\max}] \\
\lambda_{\min}(K_{dy}) &\geq \upsilon_x[\lambda_{\max}(m_y) + \lambda_{\max}(c_y)] \\
&\quad + [\Gamma_{y\max} - \lambda_{\min}(c_y)] \\
\lambda_{\max}(K_{iy}) &\leq \frac{(\lambda_{\min}(m_y))^{\frac{1}{2}}\left(\lambda_{\min}(K_{py})\right)^{\frac{3}{2}}}{6\sqrt{3}\lambda_{\max}(m_y)} \qquad (82)
\end{aligned}$$

provided that the updated law for the Fuzzy system are:

$$\begin{aligned}
\frac{d}{dt}\tilde{w}_r(z_x) &= -\frac{\rho_r}{\lambda_1}[(\dot{x} + \upsilon_x x)^T \phi_r^T(z_x)]^T \\
\frac{d}{dt}\tilde{w}_l(z_x) &= -\frac{\rho_l}{\lambda_1}[(\dot{x} + \upsilon_x x)^T \phi_l^T(z_x)]^T \\
\frac{d}{dt}\tilde{w}_r(z_y) &= -\frac{\rho_r}{\lambda_1}[(\dot{y} + \upsilon_y y)^T \phi_r^T(z_y)]^T \\
\frac{d}{dt}\tilde{w}_l(z_y) &= -\frac{\rho_l}{\lambda_1}[(\dot{y} + \upsilon_y y)^T \phi_l^T(z_y)]^T \qquad (83)
\end{aligned}$$

where ρ_r, λ_1 are positive definite matrix, $\upsilon_x > 0$ is a design parameter, $\lambda_{\min}$ and $\lambda_{\max}$ are the minimum and maximum eigenvalues.

Proof: For stability analysis, the Lyapunov candidate is selected as:

$$\begin{aligned}
V_x &= \frac{1}{2}\dot{x}^T m_x \dot{x} + \frac{1}{2}x^T K_{px} x + \frac{\upsilon_x}{2}\xi_x^{*T} K_{ix}^{-1} \xi_x^* \\
&\quad + x^T \xi_x^* + \upsilon_x x^T m_x \dot{x} + \frac{\upsilon_x}{2} x^T K_{dx} x + \int_0^t \rho_x dx \\
&\quad - k_{1x} - k_{xl}(\Delta x, \Delta y) + \frac{1}{4\rho_r}\lambda_1[\tilde{w}_r^T(z_x)\tilde{w}_r(z_x)] \\
&\quad + \frac{1}{4\rho_l}\lambda_2[\tilde{w}_l^T(z_x)\tilde{w}_l(z_x)] \qquad (84)
\end{aligned}$$

where $V_x(0) = 0$. To continue with the Lyapunov analysis, it is necessary to show that $V \geq 0$. For simplicity, V is separated into three parts as $V_x = V_1 + V_2 + V_3$, where:

$$\begin{aligned}
V_1 &= \frac{1}{6}x^T K_{px} x + \frac{\upsilon_x}{2} x^T K_{dx} x + \int_0^t \sigma_x dx \\
&\quad - k_{\sigma_{\mathbf{x}}} - \hat{f}_{xl}(\Delta x, \Delta y)\frac{1}{4\rho_r}\lambda_1[\tilde{w}_r^T(z_x)\tilde{w}_r(z_x)] \\
&\quad + \frac{1}{4\rho_l}\lambda_2[\tilde{w}_l^T(z_x)\tilde{w}_l(z_x)] \qquad (85)
\end{aligned}$$

Since $K_{px} > 0, K_{dx} > 0$, so $V_1 \geq 0$

$$V_2 = \frac{1}{6}x^T K_{px} x + \frac{\upsilon_x}{2}\xi_x^{*T} K_{ix}^{-1} \xi_x^* + x^T \xi_x^* \qquad (86)$$

When $\upsilon_x \geq \frac{3}{(\lambda_{\min}(K_{ix}^{-1})\lambda_{\min}(K_{px}))}$

$$\begin{aligned}
V_2 &\geq \frac{1}{2}\left(\sqrt{\frac{\lambda_{\min}(K_{px})}{3}}\|x\| - \sqrt{\frac{3}{(\lambda_{\min}(K_{px}))}}\left\|\xi_x^*\right\|\right)^2 \\
&\geq 0 \qquad (87)
\end{aligned}$$

And

$$V_3 = \frac{1}{6}x^T K_{px} x + \frac{1}{2}\dot{x}^T m_x \dot{x} + \upsilon_x x^T m_x \dot{x} \qquad (88)$$

Using the property of inequality

$$\begin{aligned}
A^T BC &\geq \|A\|\,\|BC\| \\
&\geq \|A\|\,\|B\|\,\|C\| \geq \lambda_{\max}(B)\|A\|\,\|C\| \\
V_3 &\geq \frac{1}{2}(\frac{1}{3}\lambda_{\min}(K_{px})\|x\|^2 \\
&\quad + \lambda_{\min}(m_x)\|\dot{x}\|^2 + 2\upsilon_x\lambda_{\max}(m_x)\|x\|\,\|\dot{x}\|) \qquad (89)
\end{aligned}$$

When $\upsilon_x \leq \frac{1}{2}\frac{\sqrt{\frac{1}{3}\lambda_{\min}(m_x)\lambda_{\min}(K_{px})}}{\lambda_{\max}(m_x)}$

$$V_3 \geq \frac{1}{2}(\sqrt{\frac{\lambda_m(K_{px})}{3}}\|x\| + \sqrt{\lambda_m(M_x)}\|\dot{x}\|)^2 \geq 0 \qquad (90)$$

Hence $V \geq 0$ Since $\lambda_{\min}(K_{ix}^{-1}) = \frac{1}{\lambda_{\max}(K_{ix})}$

$$\begin{aligned}
\frac{\sqrt{\frac{1}{3}\lambda_{\min}(m_x)}}{\lambda_{\max}(m_x)} &\geq (\frac{6\lambda_{\max}(K_{ix})}{\sqrt{\lambda_{\min}(K_{px})}})(\frac{1}{\lambda_{\min}(K_{px})}) \\
\lambda_{\max}(K_{ix}) &\leq \frac{(\lambda_{\min}(m_x))^{\frac{1}{2}}\left(\lambda_{\min}(K_{px})\right)^{\frac{3}{2}}}{6\sqrt{3}\lambda_{\max}(m_x)} \qquad (91)
\end{aligned}$$

The derivative of eqn. (84) is:

$$\begin{aligned}
\dot{V}_x &= \dot{x}^T M_x \ddot{x} + \dot{x}^T K_{px} x + \upsilon_x \frac{d}{dx}\xi_x^{*T} K_{ix}^{-1} \xi_x^* \\
&\quad + x^T \frac{d}{dx}\xi_x^* + \dot{x}^T \xi_x^* + \dot{x}^T \rho_x + \frac{\upsilon_x}{2}\dot{x}^T M_x \dot{x} \\
&\quad + \upsilon_x x^T m_x \ddot{x} + \upsilon_x \dot{x}^T m_x \dot{x} + \upsilon_x \dot{x}^T K_{dx} x \\
&\quad + \frac{1}{2\rho_r}\lambda_1[\frac{d}{dt}\tilde{w}_r^T(z_x)\tilde{w}_r(z_x)] \\
&\quad + \frac{1}{2\rho_l}\lambda_2[\frac{d}{dt}\tilde{w}_l^T(z_x)\tilde{w}_l(z_x)] \qquad (92) \\
\dot{V}_x &= \dot{x}^T[-c_x\dot{x} - k_x x - \frac{1}{2}\theta_r^T(z_x)w_r^*(z_x) \\
&\quad - \frac{1}{2}\theta_l^T(z_x)w_l^*(z_x) - \rho_x - K_{px}x - K_{dx}\dot{x} \\
&\quad - \xi_x + \rho_x(0,0) - \frac{1}{2}\theta_r^T(z_x)w_r(z_x) \\
&\quad - \frac{1}{2}\theta_l^T(z_x)w_l(z_x)] + \dot{x}^T K_{px} x \\
&\quad + \upsilon_x \frac{d}{dx}\xi_x^{*T} K_{ix}^{-1} \xi_x^* + x^T \frac{d}{dx}\xi_x^* + \dot{x}^T \xi_x^* \\
&\quad + \dot{x}^T \rho_x + \upsilon_x \dot{x}^T m_x \dot{x} + \upsilon_x \dot{x}^T K_{dx} x
\end{aligned}$$

$$
\begin{aligned}
&+\upsilon_x x^T[-c_x\dot{x}-k_x x-\frac{1}{2}\theta_r^T(z_x)w_r^*(z_x)\\
&-\frac{1}{2}\theta_l^T(z_x)w_l^*(z_x)-\rho_x-K_{px}x\\
&-K_{dx}\dot{x}-\xi_x+\rho_x(0,0)-\frac{1}{2}\theta_r^T(z_x)w_r(z_x)\\
&-\frac{1}{2}\theta_l^T(z_x)w_l(z_x)]+\frac{1}{2\rho_r}\lambda_1[\frac{d}{dt}\tilde{w}_r^T(z_x)\tilde{w}_r(z_x)]\\
&+\frac{1}{2\rho_l}\lambda_2[\frac{d}{dt}\tilde{w}_l^T(z_x)\tilde{w}_l(z_x)] \qquad (93)\\
\dot{V}_x &= \dot{x}^T[-c_x\dot{x}-k_x x-K_{px}x-K_{dx}\dot{x}\\
&-\xi_x+\rho_x(0,0)]+\dot{x}^T K_{px}x\\
&+\upsilon_x\frac{d}{dx}\xi_x^{*T}K_{ix}^{-1}\xi_x^*+x^T\frac{d}{dx}\xi_x^*\\
&+\dot{x}^T\xi_x^*+\upsilon_x\dot{x}^T m_x\dot{x}+\upsilon_x\dot{x}^T K_{dx}x\\
&+\upsilon_x x^T[-c_x\dot{x}-k_x x-\rho_x\\
&-K_{px}x-K_{dx}\dot{x}-\xi_x+\rho_x(0,0)]\\
&-\frac{1}{2}(\dot{x}^T+\upsilon_x x^T)\theta_r^T(z_x)[w_r(z_x)+w_r^*(z_x)]\\
&-\frac{1}{2}(\dot{x}^T+\upsilon_x x^T)\theta_l^T(z_x)[w_l(z_x)+w_l^*(z_x)]\\
&+\frac{1}{2\rho_r}\lambda_1[\frac{d}{dt}\tilde{w}_r^T(z_x)\tilde{w}_r(z_x)]\\
&+\frac{1}{2\rho_l}\lambda_2[\frac{d}{dt}\tilde{w}_l^T(z_x)\tilde{w}_l(z_x)] \qquad (94)
\end{aligned}
$$

If $\tilde{w}_r(z_x) = -[w_r(z_x)+w_r^*(z_x)]$, $\tilde{w}_l(z_x) = -[w_l(z_x)+w_l^*(z_x)]$ and the updated law for the Fuzzy system is selected as:

$$
\begin{aligned}
\frac{d}{dt}\tilde{w}_r(z_x) &= -\frac{\rho_r}{\lambda_1}[(\dot{x}+\upsilon_x x)^T\phi_r^T(z_x)]^T\\
\frac{d}{dt}\tilde{w}_l(z_x) &= -\frac{\rho_l}{\lambda_1}[(\dot{x}+\upsilon_x x)^T\phi_l^T(z_x)]^T \qquad (95)
\end{aligned}
$$

Then

$$
\begin{aligned}
\dot{V}_x &= \dot{x}^T[-c_x\dot{x}-k_x x-K_{px}x-K_{dx}\dot{x}\\
&-\xi_x+\rho_x(0,0)]+\dot{x}^T K_{px}x\\
&+\upsilon_x\frac{d}{dx}\xi_x^{*T}K_{ix}^{-1}\xi_x^*+x^T\frac{d}{dx}\xi_x^*+\dot{x}^T\xi_x^*\\
&+\upsilon_x\dot{x}^T m_x\dot{x}+\upsilon_x\dot{x}^T K_{dx}x\\
&+\upsilon_x x^T[-c_x\dot{x}-k_x x\\
&-\rho_x-K_{px}x-K_{dx}\dot{x}-\xi_x+\rho_x(0,0)] \qquad (96)
\end{aligned}
$$

Since, $\xi_x^* = \xi_x - \rho_x(0,0)$ and $\frac{d}{dx}\xi_x^* = K_{ix}x$, so $\frac{d}{dx}\xi_x^{*T}K_{ix}^{-1}\xi_x^* = x^T\xi_x^*$ and $x^T\frac{d}{dx}\xi_x^* = x^T K_{ix}x$ gives:

$$
\begin{aligned}
\dot{V}_x &= \dot{x}^T[-c_x\dot{x}-k_x x-K_{dx}\dot{x}]+x^T K_{ix}x\\
&+\upsilon_x\dot{x}^T m_x\dot{x}+\upsilon_x x^T[-c_x\dot{x}-k_x x\\
&-\rho_x-K_{px}x]=-\dot{x}^T[c_x\dot{x}+k_x x+K_{dx}\dot{x}\\
&-\upsilon_x m_x\dot{x}]-\upsilon_x x^T[c_x\dot{x}+k_x x+K_{px}x]\\
&+x^T K_{ix}x+\upsilon_x x^T[\rho_x(0,0)-\rho_x] \qquad (97)
\end{aligned}
$$

Using the Lipschitz condition eqn. (76), boundary condition eqn. (79) and considering $\rho_x(0,0)=0$:

$$
\upsilon_x x^T[\rho_x(0,0)-\rho_x] \le \upsilon_x k_{1x}\|x\|^2+\upsilon_x k_{xl}(\Delta x,\Delta y)\|x\|^2 \qquad (98)
$$

Applying the property $A^TB+B^TA \le A^T\Lambda A+B\Lambda^{-1}B$,

$$
-\upsilon_x x^T c_x\dot{x} \le \upsilon_x\lambda_{\max}(c_x)(x^Tx+\dot{x}^T\dot{x}) \qquad (99)
$$

Also,

$$
\begin{aligned}
-\upsilon_x\dot{x}^T k_x x &\le \Gamma_{x\max}(x^Tx+\dot{x}^T\dot{x})\\
\Gamma_{x\max} &\le \lambda_{\max}(k_x)
\end{aligned}
$$

where $\Gamma_{\max}$ is a design parameter. Using equations (80), (98) and (99):

$$
\begin{aligned}
\dot{V}_x \le\ & -\dot{x}^T[\lambda_{\min}(c_x)+\lambda_{\min}(K_{dx})\\
&-\upsilon_x\lambda_{\max}(m_x)-\Gamma_{x\max}-\upsilon_x\lambda_{\max}(c_x)]\dot{x}\\
&-x^T[\upsilon_x\lambda_{\min}(K_{px})+\upsilon_x\lambda_{\min}(k_x)\\
&-\lambda_{\max}(K_{ix})-\upsilon_x\lambda_{\max}(c_x)-\upsilon_x k_{1x}\\
&-\upsilon_x k_{xl}(\Delta x,\Delta y)-\Gamma_{x\max}]x \qquad (100)
\end{aligned}
$$

From eqn. (100), the system states will be bounded if the two mentioned conditions are satisfied:

$$
\begin{aligned}
\lambda_{\min}(c_x)+\lambda_{\min}(K_{dx}) &\ge \upsilon_x\lambda_{\max}(m_x)+\Gamma_{x\max}\\
&+\upsilon_x\lambda_{\max}(c_x)\upsilon_x[\lambda_{\min}(K_{px})+\lambda_{\min}(k_x)]\\
&\ge \lambda_{\max}(K_{ix})+\upsilon_x\lambda_{\max}(c_x)+\upsilon_x k_{1x}\\
&+\upsilon_x k_{xl}(\Delta x,\Delta y)+\Gamma_{x\max} \qquad (101)
\end{aligned}
$$

Equations (101) and (91) give the condition of stability as:

$$
\begin{aligned}
\lambda_{\min}(K_{px}) &\ge [k_{1x}+k_{xl}(\Delta x,\Delta y)+\lambda_{\max}(c_x)]\\
&+\frac{1}{\upsilon_x}[\lambda_{\max}(K_{ix})-\lambda_{\min}(k_x)+\Gamma_{x\max}]\\
\lambda_{\min}(K_{dx}) &\ge \upsilon_x[\lambda_{\max}(m_x)+\lambda_{\max}(c_x)]\\
&+[\Gamma_{x\max}-\lambda_{\min}(c_x)]\\
\lambda_{\max}(K_{ix}) &\le \frac{(\lambda_{\min}(m_x))^{\frac{1}{2}}(\lambda_{\min}(K_{px}))^{\frac{3}{2}}}{6\sqrt{3}\lambda_{\max}(m_x)} \qquad (102)
\end{aligned}
$$

Considering the similar analysis along $y-$component and since the cutting forces along $y-$component are in opposite direction to $x-$component, the stability conditions are:

$$
\begin{aligned}
\lambda_{\min}(K_{py}) &\ge [k_{1y}-k_{yl}(\Delta x,\Delta y)+\lambda_{\max}(c_y)]\\
&+\frac{1}{\upsilon_y}[\lambda_{\max}(K_{iy})-\lambda_{\min}(k_y)+\Gamma_{y\max}]\\
\lambda_{\min}(K_{dy}) &\ge \upsilon_x[\lambda_{\max}(m_y)+\lambda_{\max}(c_y)]\\
&+\left[\Gamma_{y\max}-\lambda_{\min}(c_y)\right]\lambda_{\max}(K_{iy})\\
&\le \frac{(\lambda_{\min}(m_y))^{\frac{1}{2}}\left(\lambda_{\min}(K_{py})\right)^{\frac{3}{2}}}{6\sqrt{3}\lambda_{\max}(m_y)} \qquad (103)
\end{aligned}
$$

when the updated law for the Fuzzy system along $y-$component are selected as:

$$
\begin{aligned}
\frac{d}{dt}\tilde{w}_r(z_y) &= -\frac{\rho_r}{\lambda_1}[(\dot{y}+\upsilon_y y)^T\phi_r^T(z_y)]^T\\
\frac{d}{dt}\tilde{w}_l(z_y) &= -\frac{\rho_l}{\lambda_1}[(\dot{y}+\upsilon_y y)^T\phi_l^T(z_y)]^T \qquad (104)
\end{aligned}
$$

■

VI. VALIDATION

For validation of the effectiveness of the proposed control strategy, the cutting conditions of milling process in [24] were used to simulate the milling process. The tool and cutting parameters are shown in Table 4.

TABLE 4. Milling process parameters [24] .

Parameter	Value	Units
m_x, m_y	20, 20	kg
c_x, c_y	1200, 4300	Ns/m
k_x, k_y	$(7.2, 64.8) \times 10^6$	N/m
ξ_1	6700×10^9	N/m^3
ξ_2	-4900×10^6	N/m^2
ξ_3	3000×10^3	N/m
ξ_4	1700×10^3	N
δ_1	13000×10^9	N/m^3
δ_2	-7200×10^6	N/m^2
δ_3	13	N
δ_4	25	N
n, Ω	4, 3000	rev/min

The software environment is *Matlab/Simulink*. Simulations are presented to show that the tool chatter can be attenuated to a significant level by using the *AVD* as an actuator with the developed controllers thus validating the effectiveness of the proposed control approach using *PD*, *PID*, Type-2 Fuzzy *PD* and Type-2 Fuzzy *PID*. A simulation period of 0.5 s was considered for evaluation. For the simulation purposes, the weight of the *AVD* is considered to be 5% of the structure.

Two subsytem blocks of milling model, one without control system and other with control system were created to compare the results. The cutting and damper forces are the inputs to the milling process model. The frequency for the simulation process was set at 500 rad/s. Numerical integrators were used to compute the velocity and position from the acceleration signal. Three sets of test were simulated, *PD*/*PID* controllers, *PD*/*PID* controllers along with Type-1 Fuzzy toolbox, *PD*/*PID* with open source Type-2 Fuzzy toolbox to extract the simulation results. The control signal from the controller subsystem block is fed to the *AVD* subsystem simulation block to generate the required control forces along x-direction and y-direction. IT2-*FLS* toolbox [35] is utilized to design the Type-2 Fuzzy system.

The newly developed components are functions for type-reduction operations with a brand interface. The main user interfaces of the IT2-*FLS* toolbox consist of main editor, membership function editor, rule editor and surface viewer. The membership functions of the inputs (position and velocity errors) were chosen to be as Gaussian functions as shown in Fig. 5, where mfU and mfL are the upper and lower membership functions.

For the position error, three membership functions were selected and for the velocity error, two membership functions were selected. They were normalized in $[-\mathbf{2}, \mathbf{2}]$.

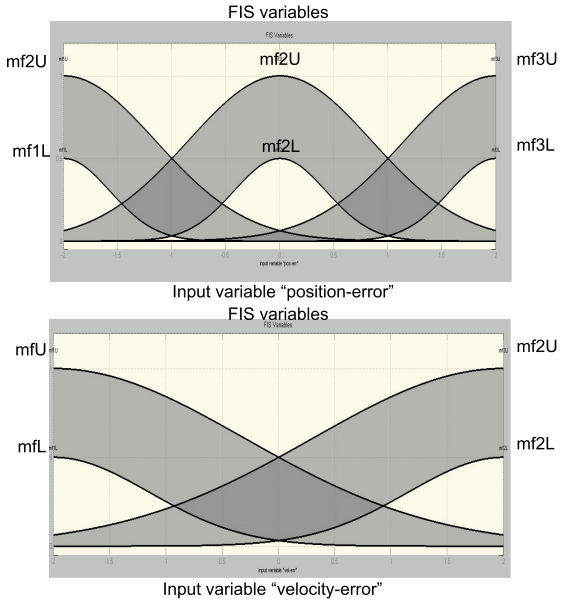

FIGURE 5. Membership functions of position error (top) and velocity error (bottom).

Reference [16] was utilized to defuzzify the Type-2 Fuzzy system. It has been noted during the analysis that the five Fuzzy rules were sufficient to maintain minimum regulation errors. For Type-1 Fuzzy system, ten IF-THEN rules were sufficient to maintain the minimum regulation error. Gaussian functions were applied for Type-1 Fuzzy system. IF-THEN rules were applied for both Type-1 and Type-2 Fuzzy system as follows:

$$IF(x_e \; is \; \Theta_1), (y_e \; is \; \Theta_2)$$
$$AND(\dot{x}_e \; is \; \Theta_3), (\dot{y}_e \; is \; \Theta_4)$$
$$THEN(u_x \; is \; \Theta_5), (u_y \; is \; \Theta_6)$$

where x_e, y_e are the position errors, $\dot{x}_e, \dot{y}_e$ are the velocity errors, and u_x, u_y are the required control forces along $x-$direction and $y-$direction. Θ_1, Θ_2, Θ_3, Θ_4, Θ_5, and Θ_6 are Type-2 Fuzzy sets. For design purposes, $\rho_r = \rho_l = 6$ and $\frac{\rho_r}{\lambda_1} = \frac{\rho_l}{\lambda_1} = 8$ were chosen.

The Theorem 1 and Theorem 2 give the sufficient conditions of the minimal proportional and derivative gains as well as maximum integral gain. The maximum and minimum bounds of the parameters were:

$$\lambda_{\max}(m_x t) = 20, \quad \lambda_{\max}(c_x) = 1.2,$$
$$\lambda_{\min}(c_x) = 1, \quad \lambda_{\min}(k_x) = 6990,$$
$$\lambda_{\max}\left(m_y\right) = 20, \quad \lambda_{\max}(c_y) = 4.3,$$
$$\lambda_{\min}(c_y) = 3.5, \quad \lambda_{\min}(k_y) = 5000,$$

k_{1x}, k_{1y}, $k_{xl}(\Delta x, \Delta y)$, $k_{yl}(\Delta x, \Delta y)$ are effected by the external force $\mathbf{F}$. The values were chosen as $k_{1x} = 250$, $k_{1y} = 250$, $k_{xl}(\Delta x, \Delta y) = 100$, $k_{xl}(\Delta x, \Delta y) = 50$ depending on the maximum values of the constant associated. The Theorem 2 gave the sufficient conditions of the minimal proportional and derivative gains and maximum integral gain.

Theorem 1 validated that both proportional and derivative gain must be positive as negative gains can make the systems unstable. For $x-$direction and $y-$direction, using the ranges from Theorem 2:

$$\lambda_{\min}(K_{px}) \geq 312, \quad \lambda_m(K_{dx}) \geq 90,$$
$$\lambda_M(K_{ix}) \leq 3112, \quad \lambda_{\min}(K_{py}) \geq 331,$$
$$\lambda_m(K_{dx}) \geq 85, \quad \lambda_M(K_{ix}) \leq 2842,$$

On the basis of eqn. (105), wide ranges of gain values were tested and it was found with several trials for *PD*, *PID*, Type-2 Fuzzy PD and Type-2 Fuzzy *PID* controllers the best selected gains for suitable vibration attenuation and stability are:

$$\lambda_{\min}(K_{px}) = 245, \quad \lambda_m(K_{dx}) = 93,$$
$$\lambda_M(K_{ix}) = 2234, \quad \lambda_{\min}(K_{py}) = 260,$$
$$\lambda_m(K_{dx}) = 88, \lambda_M(K_{ix}) = 2115$$

The comparisons in terms of vibration attenuation were carried out among *PD*, *PID*, Type-2 Fuzzy *PD* and Type-2 Fuzzy *PID* controllers. The results of these controllers were shown in Figs. 6-11. The results of the average vibration are evaluated using *Mean Squared Error* (*MSE*), $MSE = \frac{1}{d}\sum_{k=1}^{d} x(k)^2$, where $x(k)$ is the chatter vibration and d is the total number of data. Results of the average vibration are compared in Table 5.

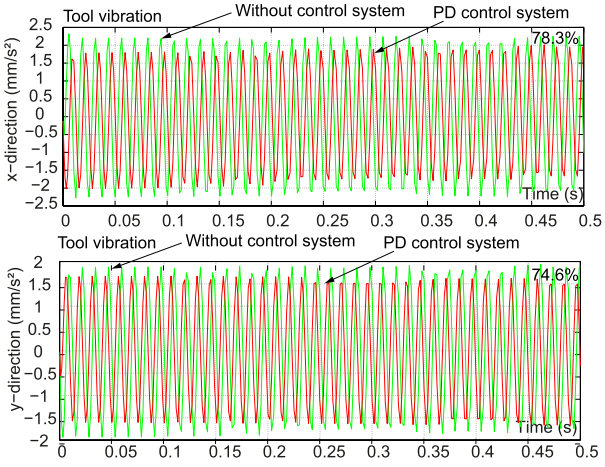

FIGURE 6. Tool vibration along x-direction (top) and y-direction (bottom) using PD controller.

Based on *MSE* indicator, the percentage vibration reduction performance of the various controllers are computed. The *PD* controller reduces the vibration in 27.2% and 25.2% along x and y directions. The percentage vibration reduction with *PID* controller was 48.9% and 34.47% along x and y directions. It is justified that although *PD* controller is able to attenuate the chatter vibration, it is not enough. This lag is somewhat achieved by introducing an integral gain to the *PD* controller. *PID* controller attenuates the chatter vibration to a better level along $x-$direction but along $y-$direction there is

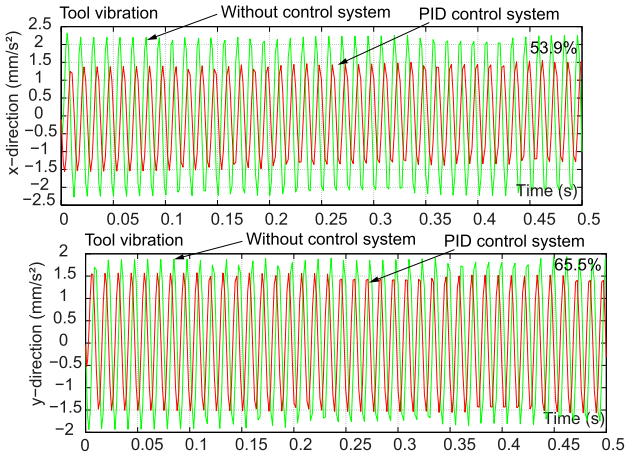

FIGURE 7. Tool vibration along x-direction (top) and y-direction (bottom) using PID controller.

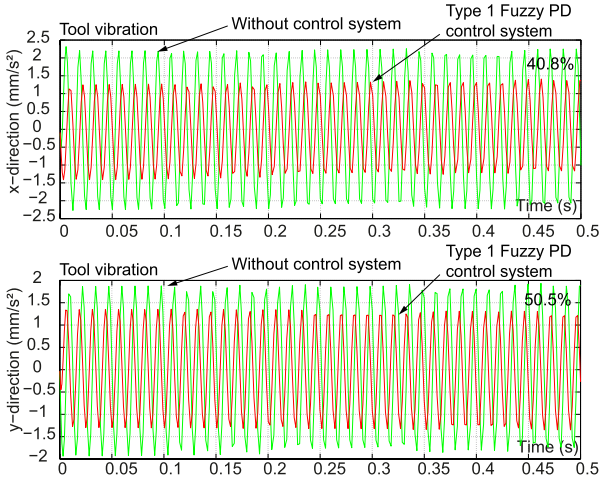

FIGURE 8. Tool vibration along x-direction (top) and y-direction (bottom) using Type-1 Fuzzy PD control system.

not much difference with *PD* controller. The performance of *PID* controller is better than *PD* controller.

The Type-1 *PD* controller reduces the vibration in 59.1% and 49.4% along x and y directions; whereas, Type-1 *PID* controller reduces the vibration in 72% and 64.4% along x and y directions. The percentage vibration reduction with Type-2 Fuzzy *PD* controller is 66.1% and 57.09% along x and y directions, and with Type-2 Fuzzy *PID* controller the percentage vibration reduction are 80.4% and 76.2% along x and y directions.

In the work of [39], the milling chatter was attenuated by proposing a *PD* control system. Although a *PD* controller is applied by considering nonlinear dynamics, the compensation of nonlinearities were not taken into consideration. In our proposal, the comparison in terms of vibration attenuation reveals the superior performance of *PD*/*PID* controller in combination with Fuzzy compensator along $x-$direction and $y-$direction. This validates that the compensation of nonlinearities with Fuzzy logic approach improves significantly

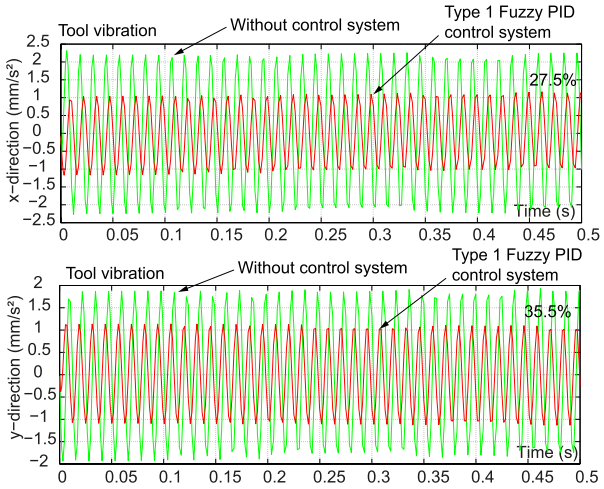

FIGURE 9. Tool vibration along x-direction (top) and y-direction (bottom) using Type-1 Fuzzy PID control system.

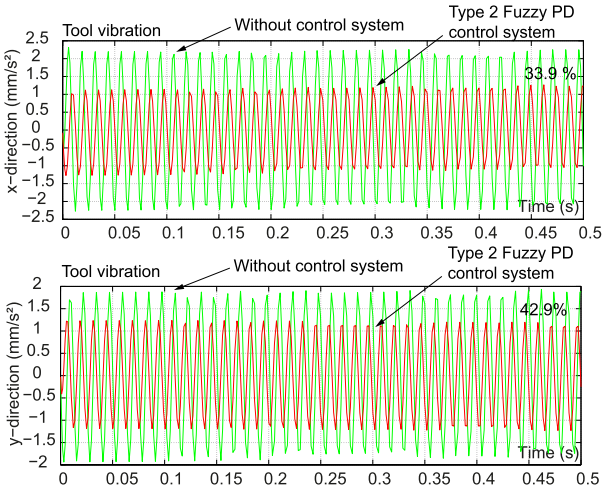

FIGURE 10. Tool vibration along x-direction (top) and y-direction (bottom) using Type-2 Fuzzy PD control system.

the performance of controllers. Several researches [17], [31] reveals that although Type-1 Fuzzy in combination with other control methodologies have been used for chatter attenuation; the combination of Fuzzy compensation with *PD*/*PID* controllers for milling chatter attenuation is investigated for the first time in this research project. Type-2 Fuzzy system performed better than Type-1 Fuzzy system which was evident from the percentage vibration attenuation results. The parameters associated to the membership functions of Type-2 Fuzzy system are l_{t2}, c_{t2}, r_{t2} and h_{t2} which define the left point, the center point, right point and the height of the membership functions. The term h_{t2} is not present in Type-1 Fuzzy system. The Type-2 Fuzzy system has more *DoF* in the design and can handle nonlinearities in a better way. From the percentage vibration attenuation, it is clear that the Type-2 Fuzzy *PID* controller outperforms all the controllers. The main constraint of the Type-2 Fuzzy toolbox is the high computational cost, this is a future work.

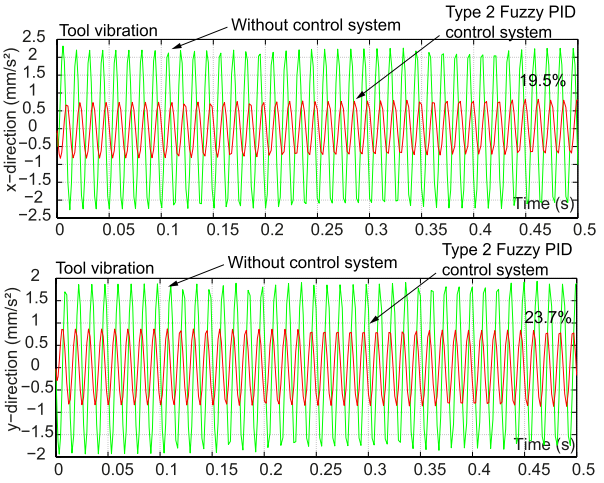

FIGURE 11. Tool vibration along x-direction (top) and y-direction (bottom) using Type-2 Fuzzy PID control system.

TABLE 5. Average vibration attenuation.

Control system	x-direction	y-direction
No controller	0.4480	0.3337
PD controller	0.3511	0.2492
PID controller	0.2418	0.2187
Type-1 Fuzzy, *PD*	0.1832	0.1688
Type-1 Fuzzy, *PID*	0.1235	0.1187
Type-2 Fuzzy, *PD*	0.1523	0.1432
Type-2 Fuzzy, *PID*	0.0877	0.0793

Reference [1] used a *PID* controller for chatter suppression; but, the stability criteria was not taken into consideration for the extraction of stable gains. In this work, from the stability view point, Theorem 1 requires that the proportional and derivative gains should be positive. In the simulations, the negative gains resulted in an unstable closed-loop operation, which is according to the conditions in Theorem 1. Theorem 2 provides sufficient conditions for the integral gains. It was found that, when integral gain is more than $3,400$ and $3,700$ along x and y direction respectively, the system becomes unstable.

The placement of damper is an important factor for suitable vibration attenuation. In this work, *AVD* was placed in the center of mass in an inclined position. The main reason for innovative placement is to make the setup a cost effective one. Since the vibration attenuation is required along both x-direction and y-direction, there is a requirement of two *AVD* placed linearly along x-component and y-component. But by placing the *AVD* in an inclined position, the control forces are resolved along x-component and y-component; instead of using two *AVD*, only one *AVD* was used, there was a cost reduction in the process and also significant vibration attenuation was observed with one *AVD* which was evident from the percentage vibration reduction results.

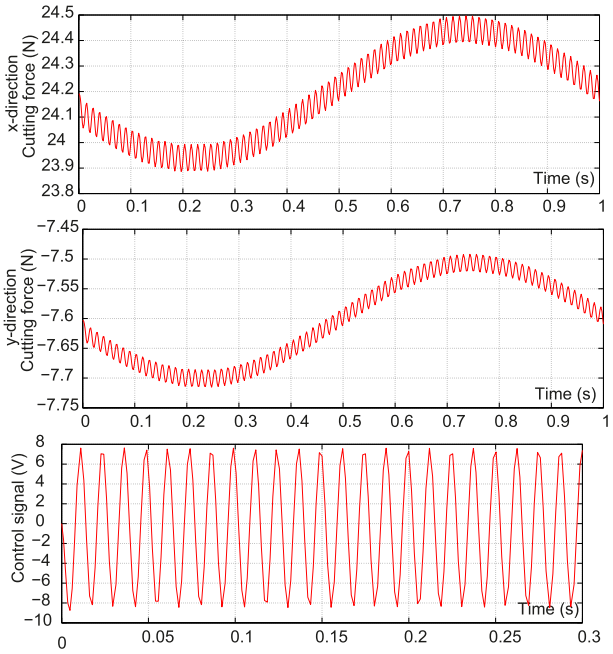

FIGURE 12. Cutting force along x-direction (top), y-direction (midle) and control signal (bottom) of Type-2 Fuzzy PID.

The cutting forces along $x-$direction and $y-$direction and the control signal of Type-2 Fuzzy *PID* are shown in Fig. 12.

VII. CONCLUSIONS

A novel active control strategy for the attenuation of chatter vibration in milling process is proposed. The important theoretical contribution associated with the stability analysis for the *PD*, *PID*, Type-2 Fuzzy *PD* and Type-2 Fuzzy *PID* was developed. The required stability conditions were obtained for the purpose of tuning the *PD/PID* gains on the basis of proposed theorems. By utilizing Lyapunov stability analysis, the minimum values of the proportional and derivative gains and the maximum values of the integral gains were computed. The Type-2 Fuzzy logic concept was utilized to compensate the nonlinearities involved within the cutting forces and damper friction. Also, Type-1 Fuzzy logic system was developed in combination with *PD/PID* controller for analyzing and comparing the performance with Type-2 Fuzzy logic system.

The numerical simulation and analysis validates the effectiveness of *PD*, *PID*, Type-1 Fuzzy *PD*, Type-1 Fuzzy *PID*, Type-2 Fuzzy *PD* and Type-2 Fuzzy *PID* controllers in the minimization of chatter vibration. Type-2 Fuzzy system performed better than Type-1 Fuzzy system due to the nature of Type-2 Fuzzy system in handling the nonlinearities with more design *DoF*. The results establish that the Type-2 Fuzzy *PID* controller is the best among all the controllers. The main contributions of this proposal are:

1) For the mitigation of milling chatter, *PD* and *PID* controllers are used in earlier research project. The stability of the controller is an important issue and needs to be dealt effectively as unstable controller may add up unnecessary forces that may result in tool damage and improper finish of the product. In this work, the stability of *PD* and *PID* controllers were validated which has not been given importance in earlier research considering milling chatter attenuation.
2) The implementation of Type-2 Fuzzy logic system with *PD/PID* controllers for the compensation of nonlinearities was carried out for the first time. The simulation results validate that a Fuzzy system can handle nonlinearities to suitable extent for increasing the effectiveness of *PD/PID* controllers.
3) The technique of active control using *AVD* placed in an effective position is entirely a new concept. The simulation results suggest that by placing the *AVD* in an inclined position and by resolving forces in two directions, suitable vibration attenuation is achieved. This innovative strategy rules out the use of multiple dampers which is advantageous from the cost point of view.

Future work is intended towards the development of the experimental setup for further investigation and the improvement of the controller by minimizing the computational cost associated with the Type-2 Fuzzy system.

REFERENCES

[1] W. N. Alharbi, A. Batako, and B. Gomm, "PID controller design for vibratory milling," in *Proc. ISER Int. Conf.*, Marrakesh, Morocco, 2017, pp. 1–4.
[2] Y. Altintas and A. Ber, "Manufacturing automation: Metal cutting mechanics, machine tool vibrations, and CNC design," *Appl. Mech.*, vol. 54, no. 5, p. B84, 2001.
[3] Y. Altintas, G. Stepan, D. Merdol, and Z. Dombovari, "Chatter stability of milling in frequency and discrete time domain," *CIRP J. Manuf. Sci. Technol.*, vol. 1, no. 1, pp. 35–44, 2008.
[4] R. I. John, P. R. Innocent, and M. R. Barnes, "Neuro-fuzzy clustering of radiographic tibia image data using type 2 fuzzy sets," *Inf. Sci.*, vol. 125, nos. 1–4, pp. 65–82, Jun. 2000.
[5] O. Castillo, L. Aguilar, N. CÃązarez, and P. Melin, "Systematic design of a stable type-2 fuzzy logic controller," in *Forging New Frontiers: Fuzzy Pioneers II*, vol. 218. Berlin, Germany: Springer, 2008.
[6] Z. Chen, H.-T. Zhang, X. Zhang, and H. Ding, "Adaptive active chatter control in milling processes," *J. Dyn. Syst., Meas., Control*, vol. 136, no. 2, p. 021007, 2014.
[7] K. De Cock, B. De Moor, W. Minten, B. W. Van, and H. Verrelst, "A tutorial on PID-control," Dept. Elect. Eng., KU Leuven, Leuven, Belgium, Tech. Rep., Aug. 1997.
[8] J. L. Dohner *et al.*, "Mitigation of chatter instabilities in milling by active structural control," *J. Sound Vib.*, vol. 269, nos. 1–2, pp. 197–211, 2004.
[9] Z. Dombovari, R. E. Wilson, and G. Stepan, "Estimates of the bistable region in metal cutting," *Proc. R. Soc. Lond. A, Math. Phys. Sci.*, vol. 464, no. 2100, pp. 3255–3271, 2008.
[10] A. Erturk and D. Inman, "Piezoelectric shunt damping for chatter suppression in machining processes," in *Proc. ISMA*, Leuven, Belgium, 2008.
[11] G. Jin, Q. Zhang, S. Hao, and Q. Xie, "Stability prediction of milling process with variable pitch cutter," *Math. Problems Eng.*, vol. 2013, Feb. 2013, Art. no. 932013.
[12] A. Ganguli, A. Deraemaeker, and A. Preumont, "Regenerative chatter reduction by active damping control," *J. Sound Vibrat.*, vol. 300, nos. 3–5, pp. 847–862, Mar. 2007.
[13] A. Harms, B. Denkena, and N. Lhermet, "Tool adaptor for active vibration control in turning operations," in *Proc. 9th Int. Conf. New Actuat.*, Bremen, Germany, 2004, pp. 694–697.

[14] T. Kalmár-Nagy, G. Stépán, and F. C. Moon, "Subcritical Hopf bifurcation in the delay equation model for machine tool vibrations," *Nonlinear Dyn.*, vol. 26, no. 2, pp. 121–142, 2001.
[15] F. L. Lewis, D. M. Dawson, and C. T. Abdallah, "Number mathematical modelling: Theory and applications," in *Robot Manipulator Control: Theory and Practice*, 2nd ed. Boca Raton, FL, USA: CRC Press, 2003.
[16] Q. Liang and J. M. Mendel, "Interval type-2 fuzzy logic systems: Theory and design," *IEEE Trans. Fuzzy Syst.*, vol. 8, no. 5, pp. 535–550, Oct. 2000.
[17] M. Liang, T. Yeap, and A. Hermansyah, "A fuzzy system for chatter suppression in end milling," *Proc. Inst. Mech. Eng. B, J. Eng. Manuf.*, vol. 218, no. 4, pp. 403–417, 2004.
[18] T.-C. Lin, H.-L. Liu, and M.-J. Kuo, "Direct adaptive interval type-2 fuzzy control of multivariable nonlinear systems," *Eng. Appl. Artif. Intell.*, vol. 22, no. 3, pp. 420–430, 2009.
[19] X. Liu, C.-Y. Su, Z. Li, and F. Yang, "Adaptive neural-network-based active control of regenerative chatter in micromilling," *IEEE Trans. Autom. Sci. Eng.*, vol. 15, no. 2, pp. 628–640, Apr. 2018.
[20] R. Lowen and A. Verschoren, Eds., *Foundations of Generic Optimization: Applications of Fuzzy Control, Genetic Algorithms and Neural Networks*, vol. 2. Berlin, Germany: Springer, 2008.
[21] S. N. Melkote and W. J. Endres, "The importance of including size effect when modeling slot milling," *J. Manuf. Sci. Eng.*, vol. 120, no. 1, pp. 68–75, 1998.
[22] J. M. Mendel, *Uncertain Rule-Based Fuzzy Systems: Introduction and New Directions*, 2nd ed. Upper Saddle River, NJ, USA: Prentice-Hall, 2001.
[23] H. Moradi, F. Bakhtiari-Nejad, M. R. Movahhedy, and G. Vossoughi, "Stability improvement and regenerative chatter suppression in nonlinear milling process via tunable vibration absorber," *J. Sound Vibrat.*, vol. 331, no. 21, pp. 4668–4690, 2012.
[24] H. Moradi, M. R. Movahhedy, and G. Vossoughi, "Dynamics of regenerative chatter and internal resonance in milling process with structural and cutting force nonlinearities," *J. Sound Vibrat.*, vol. 331, no. 16, pp. 3844–3865, 2012.
[25] H. Moradi, G. Vossoughi, M. R. Movahhedy, and H. Salarieh, "Suppression of nonlinear regenerative chatter in milling process via robust optimal control," *J. Process. Control*, vol. 23, no. 5, pp. 631–648, Jun. 2013.
[26] A. Parus, B. Powałka, K. Marchelek, S. Domek, and M. Hoffmann, "Active vibration control in milling flexible workpieces," *J. Vib. Control*, vol. 19, no. 7, pp. 1103–1120, 2013.
[27] G. Quintana and J. Ciurana, "Chatter in machining processes: A review," *Int. J. Mach. Tools Manuf.*, vol. 51, no. 5, pp. 363–376, 2011.
[28] C. Roldán, F. J. Campa, O. Altuzarra, and E. Amezua, "Automatic identification of the inertia and friction of an electromechanical actuator," in *New Advances in Mechanisms, Transmissions and Applications*, vol. 17. Dordrecht, The Netherlands: Springer, 2014, pp. 409–416.
[29] R. Rusinek, M. Wiercigroch, and P. Wahi, "Modelling of frictional chatter in metal cutting," *Int. J. Mech. Sci.*, vol. 89, pp. 167–176, Dec. 2014.
[30] R. Sepúlveda, O. Castillo, P. Melin, A. Rodríguez-Díaz, and O. Montiel, "Experimental study of intelligent controllers under uncertainty using type-1 and type-2 fuzzy logic," *Inf. Sci.*, vol. 177, no. 10, pp. 2023–2048, 2007.
[31] N. D. Sims, G. Manson, and B. Mann, "Fuzzy stability analysis of regenerative chatter in milling," *J. Sound Vibrat.*, vol. 329, no. 8, pp. 1025–1041, Apr. 2010.
[32] E. D. Sontag and Y. Wang, "On characterizations of the input-to-state stability property," *Syst. Control Lett.*, vol. 24, no. 5, pp. 351–359, 1995.
[33] J. Ssffury and E. Altus, "Chatter resistance of non-uniform turning bars with attached dynamic absorbers—Analytical approach," *J. Sound Vib.*, vol. 329, pp. 2029–2043, 2010.
[34] G. Stepan and T. Kalmar-Nagi, "Nonlinear regenerative machine tool vibrations," in *Proc. 16th ASME Biennial Conf. Mech. Vib. Noise*, Sacramento, CA, USA, 1997, pp. 1–11.
[35] A. Taskin and T. Kumbasar, "An open source MATLAB/Simulink toolbox for interval type-2 fuzzy logic systems," in *Proc. IEEE Symp Comput. Intell.*, vol. 1, Cape Town, South Africa, 2015, pp. 1561–1566.
[36] N. J. M. van Dijk, N. van de Wouw, E. J. J. Doppenberg, H. A. J. Oosterling, and H. Nijmeijer, "Robust active chatter control in the high-speed milling process," *IEEE Trans. Control Syst. Technol.*, vol. 20, no. 4, pp. 901–917, Jul. 2012.
[37] G. S. Venter and M. M. da Silva, "An analysis of surface roughness in turning/boring under different chatter conditions," in *Proc. 24th ABCM Int. Conf. Mech. Eng.*, Curitiba, Brazil, 2017.
[38] G. L. Venter, L. M. do Paraizo Silva, M. B. Carneiro, and M. M. da Silva, "Passive and active strategies using embedded piezoelectric layers to improve the stability limit in turning/boring operations," *Int. J. Adv. Manuf. Technol.*, vol. 89, nos. 9–12, pp. 2789–2801, 2017.
[39] A. Weremczuk, R. Rusinek, and J. Warminski, "The concept of active elimination of vibrations in milling process," *Procedia CIRP*, vol. 31, pp. 82–87, Jun. 2015.
[40] Y. Yang, W. Dai, and Q. Liu, "Design and implementation of two-degree-of-freedom tuned mass damper in milling vibration mitigation," *J. Sound Vib.*, vol. 335, pp. 78–88, Jan. 2015.
[41] U. Yigit, E. Cigeroglu, and E. Budak, "Chatter reduction in turning by using piezoelectric shunt circuits," in *Topics in Modal Analysis*, vol. 7. New York, NY, USA: Springer, 2014.
[42] L. Zhang and M. Z. Q. Chen, "Event-based global stabilization of linear systems via a saturated linear controller," *Int. J. Robust Nonlinear Control*, vol. 26, no. 5, pp. 1073–1091, Mar. 2016.
[43] H.-T. Zhang, Y. Wu, D. He, and H. Zhao, "Model predictive control to mitigate chatters in milling processes with input constraints," *Int. J. Mach. Tools Manuf.*, vol. 91, pp. 54–61, Apr. 2015.

SATYAM PAUL received the B.S. degree in mechanical engineering from the National Institute of Technology, Silchar, India, in 2005, the M.S. degree in mechatronics from VIT University, Vellore, India, in 2009, and the Ph.D. degree in automatic control from CINVESTAV-IPN, Mexico City, Mexico, 2017. He is currently a Post-Doctoral Researcher with the School of Engineering and Sciences, Tecnológico de Monterrey.

From 2009 to 2012, he was an Assistant Professor with the Department of Mechanical Engineering, Sikkim Manipal Institute of Technology, Rangpo, India. From 2012 to 2013, he was an Assistant Professor with the Department of Mechanical Engineering, Sir Padampat Singhania University, Udaipur, India. His research interests include vibration control, nonlinear control, stability analysis, intelligent techniques, control algorithms, system identification, and system modeling.

Dr. Paul received the Conacyt-Mexico Ph.D. Scholarship for the period 2014–2017.

RUBEN MORALES-MENENDEZ received the Ph.D. degree in artificial intelligence. He was a Visiting Scholar with the Laboratory of Computational Intelligence, The University of British Columbia, Canada. He is currently a consultant, specializing in the analysis and design of automatic control systems for continuous processes. He is also the Dean of Graduate Studies with the School of Engineering and Sciences, Tecnológico de Monterrey. He is a member of the National System of Researchers (Leve II), the Mexican Academic of Sciences, and the Academic of Engineering Mexico.